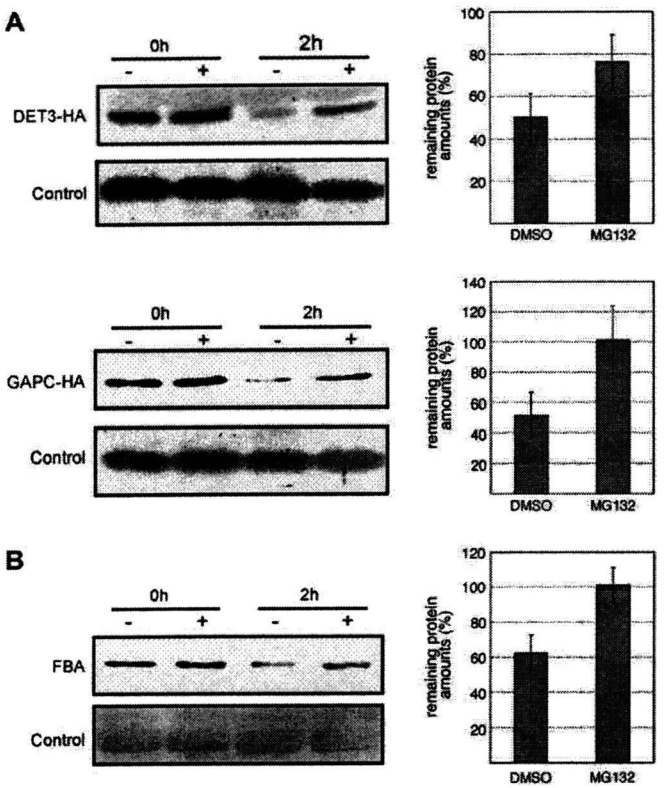

Fig. 3. Degradation assays of potential ubiquitinated proteins. Protein extracts were treated with MG132 (+) or DMSO (–). Lower panels of each figure indicate loading controls. Graphs on the right represent the relative amount of remaining protein (%) after treatment with MG132 (+) or DMSO. Error bars indicate standard deviations. (A) DET3-HA and GAPC-HA proteins transiently expressed in *N. benthamiana* leaves were detected with anti-HA antibody. (B) Total proteins were extracted from *Arabidopsis* seedlings. Immunoblot analysis was performed with anti-FBA antibody.

proteasome-dependent proteolysis. Other subunits A and B of V-ATPase were respectively isolated as ubiquitinated proteins in Maor's and Manzano's studies (Maor *et al.*, 2007; Manzano *et al.*, 2008), whereas the anti-Ub antibody used in our study could trap all of these subunits, implying that the difference in the identified subunits of V-ATPase may be attributed to the distinct specificity of the ligands used for affinity purification. It was also suggested that each subunit is ubiquitinated by a distinct ubiquitination pathway, and at least one subunit DET3 of the V-ATPase complex was degraded by the 26S proteasome.

GAPC was detected in four gel pieces, although the ubiquitination-targeting signal motif was absent (see Supplementary Table S1 at *JXB* online). The degradation of GAPC by the 26S proteasome has not been reported to date. Since it has also been reported as a ubiquitinated protein (Manzano *et al.*, 2008), the degradation by the 26S proteasome of the GAPC protein, which was transiently expressed similar to DET3, was examined. As shown in Fig. 3A, the degradation of the GAPC protein was inhibited by MG132 treatment, but not DMSO treatment, indicating that it was regulated by the Ub/proteasome-dependent proteolysis.

FBA was identified in seven gel pieces, although it did not contain any potential ubiquitination-targeting signal motifs (see Supplementary Table S1 at *JXB* online). FBA was also identified as a ubiquitinated protein (Maor *et al.*, 2007). Thus, it was expected that FBA would be degraded by the 26S proteasome. To examine the FBA degradation by the 26S proteasome in *Arabidopsis* seedlings, the protein extract was incubated with or without MG132, and FBA protein was detected with its antibody. As shown in Fig. 3B, the degradation of FBA was inhibited by MG132, demonstrating that FBA was regulated by Ub/proteasome-dependent proteolysis in *Arabidopsis* seedlings.

The degradation of DET3, GAPC, and FBA by the 26S proteasome was demonstrated for the first time in this study. GAPC and FBA are involved in glycolysis and are known to respond to environmental stress. Thus, the turnover of these proteins may be regulated by the Ub/proteasome-dependent proteolysis in the glycolytic pathway and/or stress response. It would be interesting to investigate the contribution of Ub-mediated regulation of these proteins in metabolism and/or stress response as a future work.

Conclusions

This study showed the Ub-related proteome of *Arabidopsis* seedlings. Protein purification under native conditions with an anti-Ub antibody contributed to the isolation of various Ub-related proteins that mainly comprised proteins involved in Ub/proteasome-dependent proteolysis. The protein population identified contained both the targets of ubiquitination and their associated proteins. Biochemical evidence is required to characterize exactly which protein is the direct target of ubiquitination. Nevertheless, classification of the identified proteins based on the potential ubiquitination-targeting signal motifs, in-gel mobilities, and the previous reports contributed to the prediction of ubiquitinated proteins and their associated proteins. Our results are expected to be of use to the future investigation of Ub-mediated protein regulation in plants.

Supplementary data

Supplementary data are available at *JXB* online.

Supplementary Fig. S1. Respective SDS-PAGE images of proteins immunopurified with FK2 obtained from three independent experiments (Ex1, Ex2, and Ex3). The staining pattern of the purified proteins was reproducible.

Supplementary Table S1. Ub-related proteins identified from *Arabidopsis* seedlings.

Supplementary Table S2. Proteins containing potential ubiquitination-targeting signal motifs for Ub/proteasome-dependent proteolysis.

Acknowledgements

We thank Dr T Nakagawa (Shimane University, Japan) for pGWB14 vector and Ms R Okanami for technical assistance. This work was supported by KAKENHI (19658041), a Grant-in-Aid for Exploratory Research from the Japan Society for the Promotion of Science (JSPS), and a Grant-in-Aid for Scientific Research from the Nara Institute of Science and Technology supported by the Ministry of Education, Culture, Sports, Science, and Technology, Japan.

References

Bachmair A, Novatchkova M, Potuschak T, Eisenhaber F. 2001. Ubiquitylation in plants: a post-genomic look at a post-translational modification. *Trends in Plant Science* **6,** 463–470.

Fujimuro M, Sawada H, Yokosawa H. 1994. Production and characterization of monoclonal antibodies specific to multi-ubiquitin chains of polyubiquitinated proteins. *FEBS Letters* **349,** 173–180.

Fujiwara M, Umemura K, Kawasaki T, Shimamoto K. 2006. Proteomics of Rac GTPase signaling reveals its predominant role in elicitor-induced defense response of cultured rice cells. *Plant Physiology* **140,** 734–745.

Haglund K, Dikic I. 2005. Ubiquitylation and cell signaling. *EMBO Journal* **24,** 3353–3359.

Hatfield PM, Gosink MM, Carpenter TB, Vierstra RD. 1997. The ubiquitin-activating enzyme (E1) gene family in *Arabidopsis thaliana*. *The Plant Journal* **11,** 213–226.

Hatakeyama S, Matsumoto M, Nakayama KI. 2005. Mapping of ubiquitination sites on target proteins. *Methods in Enzymology* **399,** 277–286.

Hershko A, Ciechanover A. 1998. The ubiquitin system. *Annual Review of Biochemistry* **67,** 425–479.

Jeon HB, Choi ES, Yoon JH, Hwang JH, Chang JW, Lee EK, Choi HW, Park ZY, Yoo YJ. 2007. A proteomics approach to identify the ubiquitinated proteins in mouse heart. *Biochemical and Biophysical Research Communications* **357,** 731–736.

Katou S, Karita E, Yamakawa H, Seo S, Mitsuhara I, Kuchitsu K, Ohashi Y. 2005. Catalytic activation of the plant MAPK phosphatase NtMKP1 by its physiological substrate salicylic acid-induced protein kinase but not by calmodulins. *Journal of Biological Chemistry* **280,** 39569–39581.

King RW, Glotzer M, Kirschner MW. 1996. Mutagenic analysis of the destruction signal of mitotic cyclins and structural characterization of ubiquitinated intermediates. *Molecular Biology of the Cell* **7,** 1343–1357.

Kraft C, Deplazes A, Sohrmann M, Peter M. 2008. Mature ribosomes are selectively degraded upon starvation by an autophagy pathway requiring the Ubp3p/Bre5p ubiquitin protease. *Nature Cell Biology* **10,** 602–610.

Kraft E, Stone SL, Ma L, Su N, Gao Y, Lau OS, Deng XW, Callis J. 2005. Genome analysis and functional characterization of the E2 and RING-type E3 ligase ubiquitination enzymes of Arabidopsis. *Plant Physiology* **139,** 1597–1611.

Manzano C, Abraham Z, López-Torrejón G, Del Pozo JC. 2008. Identification of ubiquitinated proteins in Arabidopsis. *Plant Molecular Biology* **68,** 145–158.

Maor R, Jones A, Nühse TS, Studholme DJ, Peck SC, Shirasu K. 2007. Multidimensional protein identification technology (MudPIT) analysis of ubiquitinated proteins in plants. *Molecular and Cellular Proteomics* **6,** 601–610.

Matsumoto M, Hatakeyama S, Oyamada K, Oda Y, Nishimura T, Nakayama KI. 2005. Large-scale analysis of the human ubiquitin-related proteome. *Proteomics* **5,** 4145–4151.

Mazzucotelli E, Belloni S, Marone D, De Leonardis AM, Guerra D, Di Fonzo N, Cattivelli L, Mastrangelo AM. 2006. The e3 ubiquitin ligase gene family in plants: regulation by degradation. *Current Genomics* **7,** 509–522.

Nakagawa T, Kurose T, Hino T, Tanaka K, Kawamukai M, Niwa Y, Toyooka K, Matsuoka K, Jinbo T, Kimura T. 2007. Development of series of gateway binary vectors, pGWBs, for realizing efficient construction of fusion genes for plant transformation. *Journal of Bioscience and Bioengineering* **104,** 34–41.

Nakashima A, Chen L, Thao NP, Fujiwara M, Wong HL, Kuwano M, Umemura K, Shirasu K, Kawasaki T, Shimamoto K. 2008. RACK1 functions in rice innate immunity by interacting with the Rac1 immune complex. *The Plant Cell* **20,** 2265–2279.

Peng J, Schwartz D, Elias JE, Thoreen CC, Cheng D, Marsischky G, Roelofs J, Finley D, Gygi SP. 2003. A proteomics approach to understanding protein ubiquitination. *Nature Biotechnology* **21,** 921–926.

Pfleger CM, Kirschner MW. 2000. The KEN box: an APC recognition signal distinct from the D box targeted by Cdh1. *Genes and Development* **14,** 655–665.

Pickart CM. 2001. Mechanisms underlying ubiquitination. *Annual Review of Biochemistry* **70,** 503–533.

Schumacher K, Vafeados D, McCarthy M, Sze H, Wilkins T, Chory J. 1999. The *Arabidopsis det3* mutant reveals a central role for the vacuolar H^+-ATPase in plant growth and development. *Genes and Development* **13,** 3259–3270.

Sze H, Schumacher K, Müller ML, Padmanaban S, Taiz L. 2002. A simple nomenclature for a complex proton pump: VHA genes encode the vacuolar H^+-ATPase. *Trends in Plant Science* **7,** 157–161.

Thrower JS, Hoffman L, Rechsteiner M, Pickart CM. 2000. Recognition of the polyubiquitin proteolytic signal. *EMBO Journal* **19,** 94–102.

Yanagawa Y, Sullivan JA, Komatsu S, *et al.* 2004. *Arabidopsis* COP10 forms a complex with DDB1 and DET1 *in vivo* and enhances the activity of ubiquitin conjugating enzymes. *Genes and Development* **18,** 2172–2181.

BMC Plant Biology

BioMed Central

Methodology article

Open Access

A simple and high-sensitivity method for analysis of ubiquitination and polyubiquitination based on wheat cell-free protein synthesis

Hirotaka Takahashi[1,2], Akira Nozawa[1,2,5], Motoaki Seki[3], Kazuo Shinozaki[4], Yaeta Endo*[1,2,5] and Tatsuya Sawasaki*[1,2,5]

Address: [1]Cell-Free Science and Technology Research Center, Ehime University, Matsuyama 790-8577, Japan, [2]The Venture Business laboratory, Ehime University, Matsuyama 790-8577, Japan, [3]Plant Functional Genomics Research Group, 1-7-22 Suehiro-cho, Tsurumi-ku, Yokohama, Kanagawa 230-0045, Japan, [4]Gene Discovery Research Group, RIKEN Plant Science Center, 1-7-22 Suehiro-cho, Tsurumi-ku, Yokohama, Kanagawa 230-0045, Japan and [5]RIKEN Genomic Sciences Center, 1-7-22 Suehiro-cho, Tsurumi-ku, Yokohama, Kanagawa 230-0045, Japan

Email: Hirotaka Takahashi - h-takahashi@ccr.ehime-u.ac.jp; Akira Nozawa - anozawa@ccr.ehime-u.ac.jp; Motoaki Seki - mseki@psc.riken.jp; Kazuo Shinozaki - sinozaki@rtc.riken.jp; Yaeta Endo* - yendo@eng.ehime-u.ac.jp; Tatsuya Sawasaki* - sawasaki@eng.ehime-u.ac.jp

* Corresponding authors

Published: 6 April 2009

BMC Plant Biology 2009, 9:39 doi:10.1186/1471-2229-9-39

Received: 26 December 2008
Accepted: 6 April 2009

This article is available from: http://www.biomedcentral.com/1471-2229/9/39

Abstract

Background: Ubiquitination is mediated by the sequential action of at least three enzymes: the E1 (ubiquitin-activating enzyme), E2 (ubiquitin-conjugating enzyme) and E3 (ubiquitin ligase) proteins. Polyubiquitination of target proteins is also implicated in several critical cellular processes. Although Arabidopsis genome research has estimated more than 1,300 proteins involved in ubiquitination, little is known about the biochemical functions of these proteins. Here we demonstrate a novel, simple and high-sensitive method for *in vitro* analysis of ubiquitination and polyubiquitination based on wheat cell-free protein synthesis and luminescent detection.

Results: Using wheat cell-free synthesis, 11 E3 proteins from Arabidopsis full-length cDNA templates were produced. These proteins were analyzed either in the translation mixture or purified recombinant protein from the translation mixture. In our luminescent method using FLAG- or His-tagged and biotinylated ubiquitins, the polyubiquitin chain on AtUBC22, UPL5 and UPL7 (HECT) and CIP8 (RING) was detected. Also, binding of ubiquitin to these proteins was detected using biotinylated ubiquitin and FLAG-tagged recombinant protein. Furthermore, screening of the RING 6 subgroup demonstrated that At1g55530 was capable of polyubiquitin chain formation like CIP8. Interestingly, these ubiquitinations were carried out without the addition of exogenous E1 and/or E2 proteins, indicating that these enzymes were endogenous to the wheat cell-free system. The amount of polyubiquitinated proteins in the crude translation reaction mixture was unaffected by treatment with MG132, suggesting that our system does not contain 26S proteasome-dependent protein degradation activity.

Conclusion: In this study, we developed a simple wheat cell-free based luminescence method that could be a powerful tool for comprehensive ubiquitination analysis.

Background

Protein ubiquitination plays a crucial role in numerous cellular processes such as cell growth, regulation of diverse signal transduction and disease [1-3]. The covalent attachment of ubiquitin to protein substrates requires a stepwise cascade of enzymatic reactions. First, ubiquitin is activated by E1 (ubiquitin-activating enzyme, UBA) in an ATP-dependent manner by forming a high-energy thioester-bond between the carboxyl-terminal glycine residue of ubiquitin and a cysteine residue of E1. The activated ubiquitin is then transferred to the core-cysteine residue of E2 (ubiquitin-conjugating enzyme, UBC). Together with an E3 ligase enzyme, ubiquitin is attached via its carboxyl-terminus to an e-amino group of a lysine residue in the target protein. Since E3 binds to both E2 and the target protein, and acts as scaffold between E2 and the substrate protein, the E3 ligase is the major determinant for selecting target proteins for ubiquitination. There is large number of genes encoding E3 ligases in all eukaryotes, and the diversity of E3s is thought to contribute to the substrate specificity of numerous target proteins. E3 ligases are structurally divided into three groups: HECT, RING and U-box [4]. The HECT-type E3 ligase is distinct from the other two ligases in that it forms a thioester-bond with ubiquitin prior to the transfer of ubiquitin to target proteins. The RING-type E3 ligase contains a unique domain similar to the zinc finger motif that mediates protein-protein interactions [5] and is further divided into two classes: one that can function alone and another that forms a complex with other E3 components [4].

Recent studies have shown that attachment of polyubiquitin chains on target proteins linked via lysine-48 of ubiquitin typically leads to degradation by the 26S proteasome [6], whereas linkage via lysine-63 mediates different pathways such as internalization of membrane proteins, activation of signal transduction and DNA damage repair [7]. The formation of lysyl-63-linked polyubiquitin chains is generated by specific combinations of E2s and E2 variants, which are similar to E2s except that they lack core cysteine residues required for E2 activity [8,9]. In addition, ubiquitination of substrates without polymerization, mono-ubiquitination, acts as a sorting signal for protein endocytosis and as a regulation factor for diverse proteins, including histones and transcription factors [10].

In plant, genomic research of the model plant *Arabidopsis thaliana* showed that there are two E1s, 37 E2s and more than 1,300 predicted E3s [11]. Although little is known about protein ubiquitination in plants compared with yeast and mammals, recent studies revealed that the plant ubiquitination pathway is involved in the regulation of morphogenesis, the circadian clock and responding to hormone or pathogen signal molecules [12-15]. Despite the importance of ubiquitination in plants, much of the plant ubiquitination cascade is still unknown because of its complexity and the issues inherent to the use of Arabidopsis plants for biochemical analysis. Although several interactions between E2s and RING type E3s have been demonstrated *in vitro* using recombinant proteins expressed in *Escherichia coli*, these efforts are hampered by the inability to obtain functional protein using conventional methods [16].

With this in mind, we sought to develop a novel *in vitro* method to analyze the ubiquitin pathway genome-wide. The two major obstacles hindering the development of an *in vitro* assay for genome-wide screening are the difficulty of efficiently producing recombinant protein and the inability to detect ubiquitination in a high-throughput fashion. To address the first problem we used the wheat cell-free protein synthesis system, which has been previously reported to produce a wide range of functional Arabidopsis and human proteins [17-19]. Moreover, a collection of RIKEN Arabidopsis Full Length (RAFL) cDNA clones covering about 70% of Arabidopsis genes is available [20]. Using these RAFL clones as templates, recombinant proteins involved in the ubiquitination pathway were expressed in the wheat cell-free system and used for several functional analyses. For screening, conventional detection methods such as immunoblot analysis or radioisotope-labeled proteins are not suitable for the detection of a large number of ubiquitination reactions. Recently, a high-throughput luminescence method to detect protein ubiquitination was reported [21], however this method requires purified protein and creation of specialized vectors to produce proteins. In this study, a novel *in vitro* assay to detect polyubiquitin chain formation was developed using wheat cell-free synthesis and a modified luminescence-based detection method. We demonstrate (1) creation of a simple *in vitro* method to detect polyubiquitination using crude recombinant E3s, (2) discovery of the activity of At1g55530 by screening a RING subgroup in the reported assay, and (3) the polyubiquitination assay in the presence of MG132 demonstrated the absence of 26S proteasome-dependent protein degradation activity in wheat cell-free system.

Results

Detection of Polyubiquitin Chains on AtUBC22 E2 enzyme

Recently, AtUBC22 (At5g05080) E2 protein has been shown to catalyze polyubiquitin chain formation without an E3 ligase, although AtUBC35 (At1g78870) E3-independent polyubiquitination activity could not be detected [16]. We employed AtUBC22 and AtUBC35 as model E2 proteins to develop a novel polyubiquitination assay. We have also demonstrated that addition of biotin ligase (BirA) and biotin to the wheat cell-free protein production system yields a single biotinylation on a target pro-

tein containing a biotin ligation site [22]. Using this method, biotinylated recombinant AtUBC22 and AtUBC35 were synthesized and, without purification from the translation mixture, the polyubiquitination reaction was performed on the crude recombinant protein. After the reaction, biotinylated AtUBC22 and AtUBC35 were purified using streptavidin-conjugated magnetic beads and the polyubiquitin chain was detected by immunoblot analysis. As shown in Fig 1A, AtUBC22 showed polyubiquitination, whereas AtUBC35 showed mainly monoubiquitination. Interestingly, both E2s still had activity in absence of exogenous E1 in polyubiquitin reaction mixture (Fig. 1A, middle lanes), suggesting that wheat cell-free system has high endogenous E1 activity.

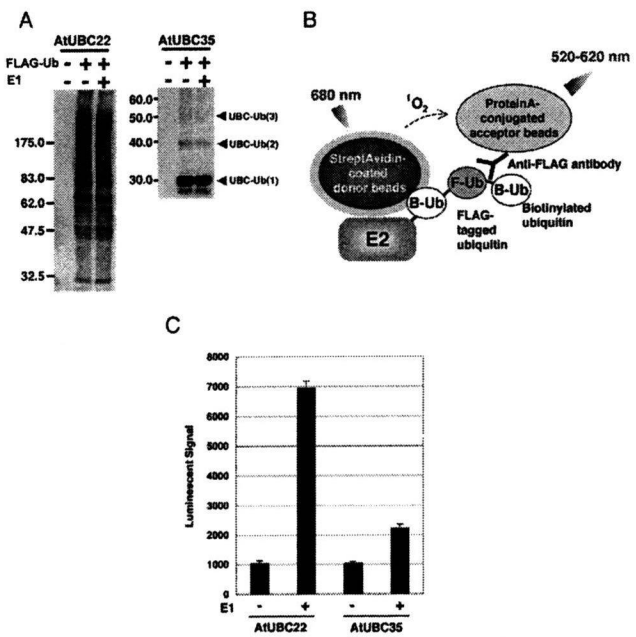

Figure 1
Detection of E3-independent polyubiquitination of AtUBC22 by luminescent analysis. A, Polyubiquitin chain on AtUBC22 but not on AtUBC35 was detected by immunoblot analysis. In this assay, polyubiquitination reaction was carried out with FLAG-tagged ubiquitin, and detected by immunoblot analysis using anti-FLAG antibody. B, Schematic diagram of detection of polyubiquitin chains by luminescent analysis. Protein A-conjugated acceptor beads and streptavidin-coated donor beads are bound to anti-FLAG antibody bound to FLAG-tagged ubiquitin and biotinylated E2, respectively, and these two beads are in closed proximity when polyubiquitin chain formed. Upon excitation 680 nm, a singlet oxygen is generated from the donor beads, and then transferred to the acceptor beads within 200 nm, and the singlet oxygen reacts the acceptor beads which in turn emits light at 520–620 nm. This light is measured by AlphaScreen kit and change to signal value. C, Polyubiquitin chain on purified recombinant E2 was detected by luminescent analysis in the presence (E1 +) or absence (E1 -) of exogenous E1. Error bars represent standard deviations from three independent experiments.

While immunoblot analysis is an excellent detection method, it is not suitable for high-throughput detection of numerous polyubiquitination reactions. Initially, we attempted to use luminescent analysis, based on the AlphaScreen technology, to detect the polyubiquitination activity of AtUBC22 and AtUBC35. In principle, if a polyubiquitin chain is formed by FLAG-tagged and biotinylated ubiquitins, it will bring into proximity the streptavidin-coated donor bead (bound to biotin) and the protein A-conjugated acceptor bead (bound to anti-FLAG IgG), producing a luminescent signal (Fig. 1B). Considering that the wheat cell-free system has high endogenous E1 activity (Fig. 1A), it may also have endogenous E2 and E3 activity. In order to avoid formation of polyubiquitin chains by an endogenous wheat germ ubiquitin pathway, purified E2s were used in this assay. As shown in Fig 1C, high luminescent signal was observed in the presence of AtUBC22 in E1-dependent manner. In contrast, AtUBC35 showed low signal. The two luminescent signals were approximately consistent with immunoblot data that AtUBC22 and AtUBC35 have high and low polyubiquitination activities respectively, as demonstrated in Fig 1A. These results indicate that the luminescent method can detect polyubiquitin chain formation by using the two types of ubiquitins.

Ubiquitination and Polyubiquitination Analyses of HECT-TypeE3 Ligases

Polyubiquitination activity of E3 ligases activated by the step-wise E1 to E3 cascade is well documented [3]. We next attempted to reconstruct this cascade *in vitro* and to detect the E3-formed polyubiquitin chains using our luminescent method. Due to the size of HECT-type E3 ligases, ranging from 100 to 428 kDa in Arabidopsis, production of active protein by traditional expression methods may not be easy and biochemical analysis using only truncated recombinant protein has been carried out previously [23]. We attempted to produce full-length Arabidopsis HECT-type E3 ligase proteins using the wheat cell-free system and monitored ubiquitin-conjugation and polyubiquitination by luminescence. Two genes that encode Arabidopsis HECT-type E3 ligase, *UPL5* and *UPL7* [24], were analyzed in this study. We obtained UPL5 and UPL7 cDNA from the RAFL library and produced FLAG-tagged protein in the wheat cell-free system. Ubiquitination of FLAG-labeled UPLs (UPL-FLAGs) was investigated by both the luminescent and immunoblot methods. The successful production of the two recombinant HECT proteins was observed by immunoblot analysis (Fig. 2A) and used in the luminescence assay without purification. To detect ubiquitination of the HECT proteins, UPL-FLAGs

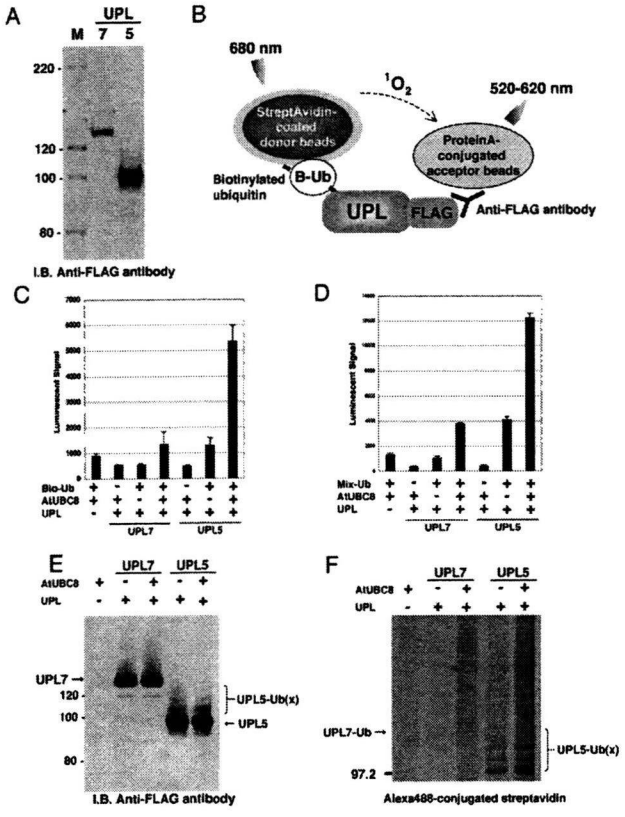

Figure 2

Analysis of recombinant Arabidopsis HECT-type E3 ligases (UPL7 and UPL5). A, Production of FLAG-tagged recombinant UPL proteins was detected by immunoblot analysis. For analysis, 5 μl of crude recombinant UPL proteins were loaded, and detected by immunoblot analysis using anti-FLAG antibody. B, Schematic diagram of detection of ubiquitin-conjugation of UPLs by luminescent analysis. Protein A-conjugated acceptor beads and streptavidin-coated donor beads were bound to anti-FLAG antibody bound to FLAG-tagged recombinant UPLs and biotinylated ubiquitin, respectively, and detected by same principle and procedure described in Figure 1B. C, The ubiquitination of crude recombinant UPL7 and UPL5 was detected by luminescent analysis described in B. Bio-Ub means biotinylated ubiquitin. D, polyubiquitination of crude recombinant UPL7 and UPL5 was detected by luminescent analysis with anti-His antibody. Mix-Ub indicated the mixture of His-tagged and biotinylated ubiquitin. E and F, Mobility shift of UPLs (E) and formation of polyubiquitin chains (F) were detected by immunoblot using anti-FLAG antibody and Alexa488-conjugated streptavidin, respectively. The polyubiquitination reaction was done with FLAG-tagged recombinant UPLs in presence or absence of crude AtUBC8, and then recombinant UPLs were purified by anti-FLAG antibody-conjugated agarose. Error bars represent standard deviations from three independent experiments.

and biotinylated ubiquitin were used. When biotinylated ubiquitin is conjugated to the UPL-FLAG, a high luminescent signal is obtained (Fig. 2B). As a result of the analysis, ubiquitin-conjugation of UPL5 was observed (Fig. 2C). In addition, polyubiquitin chains formed by UPLs were detected with the luminescence assay using His-tagged and biotinylated ubiquitin. To subtract polyubiquitin chain formation from endogenous E2 and E3 in wheat cell-free system, the assay was performed without recombinant UPL and only low signal was detected (Fig. 2D, "UPL-" lane). As expected, luminescent signal was observed in recombinant UPL5 and UPL7 (Fig. 2D). Although the luminescent signal of UPL7 was lower than that of UPL5, the signal was still two-fold higher than the endogenous background signal. These results were confirmed by immunoblot analysis that showed distinct mobility shifts of UPL5 (Fig. 2E) when detecting FLAG-tagged UPLs, and polyubiquitin chain formation of UPL5 monitoring Alexa488-conjugated streptavidin (Fig. 2F). Comparing the amount of polyubiquitin chain formation in absence of UPLs (Fig. 2F, "UPL-" lane), UPL7 formed weak but distinct polyubiquitin chains in presence of AtUBC8. These luminescent signals were consistent with immunoblot data. Interestingly, polyubiquitin chains were formed by UPL5 without supplementing exogenous E2 protein (Fig. 2D and 2F, "AtUBC8-" lane), suggesting that wheat germ extract has endogenous E2 activity as well as endogenous E1 activity. These data indicate that the wheat cell-free production system is able to produce high molecular weight proteins in functional forms and that our luminescence method can detect activity of HECT-type E3 ligases without purification. This is the first data showing that full length recombinant HECT-type E3s have ubiquitin-conjugating and polyubiquitination activity. Taken together, the luminescent method based on the wheat cell-free system could be useful for biochemical analysis of HECT-type E3 ligases.

Detection of Polyubiquitin Chains by RING-Type CIP8 E3 Ligase

It is reported that at least 469 predicted RING-type E3 ligases are encoded in the Arabidopsis genome [25]. Like the HECT-type E3, we attempted to express and carry out the functional analysis of the RING-type E3 ligases. In this study, we selected CIP8 as a model RING-type E3 ligase, which is reported to possess a RING finger motif and have typical features of an E3 ligase [26]. At first, polyubiquitination activity of purified CIP8 in presence or absence of exogenous E1 and purified E2 (AtUBC8) was investigated by luminescence. As shown in Fig 3A, luminescence analysis using His-tagged and biotinylated ubiquitin showed the polyubiquitination of purified CIP8 only when exogenous E1 and purified E2 were added to the reaction mixture. The CIP8-dependent polyubiquitination was

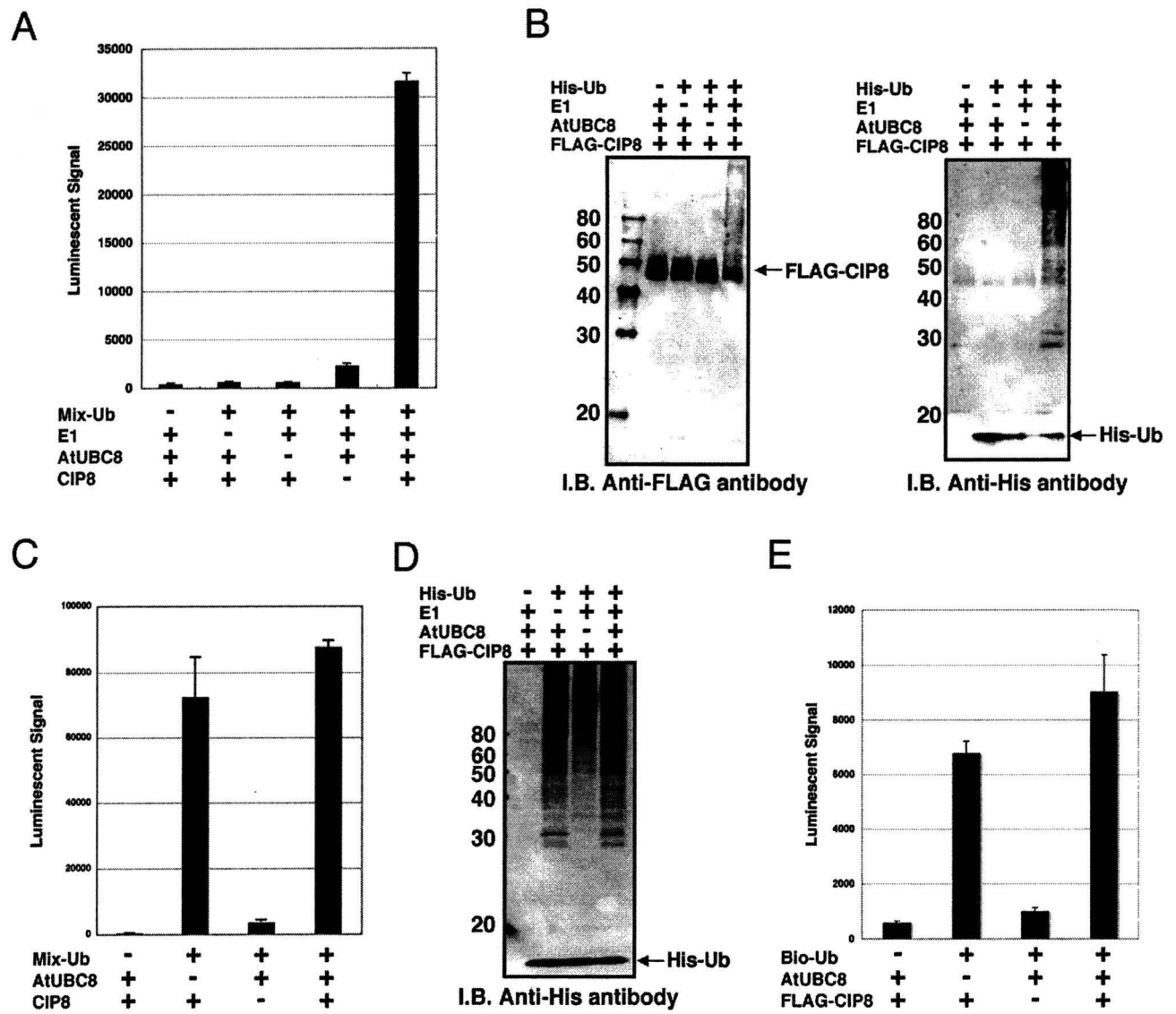

Figure 3

Detection of polyubiquitination and self-ubiquitination of CIP8. A to D, The polyubiquitination assay was carried out with purified (A and B) or crude recombinant CIP8 (C and D) and detected by luminescent analysis with anti-FLAG antibody (A and C) and immunoblot analysis (B and D). His-Ub or Mix-Ub indicate His-tagged ubiquitin or the mixture of FLAG-tagged and biotinylated ubiquitin, respectively. The polyubiquitination assay using luminescent analysis was carried out with recombinant CIP8 without tag in the presence or absence of ubiquitin related components indicated below each graph. E, Ubiquitination of crude recombinant CIP8 was observed by luminescent analysis with anti-FLAG antibody. The assay was carried out with or without biotinylated ubiquitin and crude AtUBC8 recombinant protein. Bio-Ub means biotinylated ubiquitin. Error bars represent standard deviations from three independent experiments.

confirmed by immunoblot analyses detecting both FLAG-CIP8 and His-tagged ubiquitin (Fig. 3B). On the other hand, luminescent analysis with crude CIP8 protein showed high polyubiquitination activity both in the presence or absence of purified E2 (Fig. 3C), and was confirmed by immunoblot analysis with crude protein (Fig. 3D). These data indicated that, like recombinant UPL5, crude CIP8 also utilized endogenous wheat extract E1 and E2 proteins, and therefore we could carry out the simple polyubiquitination analysis of E3 without addition of exogenous E1 and E2 proteins. Furthermore, immunoblot analysis detecting purified CIP8 (Fig. 3B) showed a mobility shift of FLAG-tagged CIP8 to higher molecular weights due to ubiquitination, whereas the mobility of the E2 was

not altered (data not shown). This result indicates that the CIP8-dependent polyubiquitin chains might be elongated on CIP8 itself. This data is consistent with a recent report showing that TRIM5a, a typical RING-type E3 ligase in human, also undergoes self-ubiquitination, forming polyubiquitin chains on itself [27]. To clarify whether the mobility shift of CIP8 was concomitant with polyubiquitin chain formation resulting from self-ubiquitination, we tried to detect ubiquitination of CIP8 by the luminescent method using crude FLAG-CIP8 protein and biotinylated ubiquitin. The luminescent method clearly detected the binding of biotinylated ubiquitin to FLAG-tagged CIP8 both in the presence and absence of exogenous E2 (Fig. 3E). Similar to polyubiquitin formation, the ubiquitination of CIP8 also occurred without the addition of exogenous E2 protein (Fig. 3E, "AtUBC8-" lane). Taken together, these data demonstrate that the luminescent method could detect formation of RING-type CIP8-dependent polyubiquitin chains and self-ubiquitination of crude CIP8.

Screening of RING-Type E3 Ligases Having Polyubiquitination Activity

Recent papers have reported that the polyubiquitin chain is an important biological regulator. Identification of activity and features of E3 ligases offers important information about the ubiquitin-dependent regulation system. Our luminescent method based on the wheat cell-free system produced a simple and high-sensitivity detection of CIP8-dependent polyubiquitin chains without any purification (Fig. 3C). Using these tools, we screened new E3 ligases for the ability to form polyubiquitin chains like CIP8.

The RING-type E3 ligases in Arabidopsis were divided into 30 subgroups based on domain structure, and CIP8 is categorized into subgroup 6 as it contains a coiled-coil domain [25]. Eight other RING-type E3s from subgroup 6 were selected for screening, and the simple polyubiquitination assay was carried out with FLAG-tagged and biotinylated ubiquitins, and the crude recombinant RING-type E3s without addition of exogenous E1 and E2. The screening result showed significant polyubiquitination activity of At1g55530, whereas other RING-E3 proteins were not active (Fig. 4A). Immunoblot analysis of purified recombinant At1g55530 confirmed the polyubiquitination activity and indicated that At1g55530 was self-ubiquitinated (Fig. 4B). The polyubiquitination activity of At1g55530 suggests that it may have a biological role for proteasome-mediated degradation like CIP8 [26]. These results show that the wheat cell-free protein expression system and the luminescent ubiquitination detection method could support functional high-throughput screening of E3 proteins.

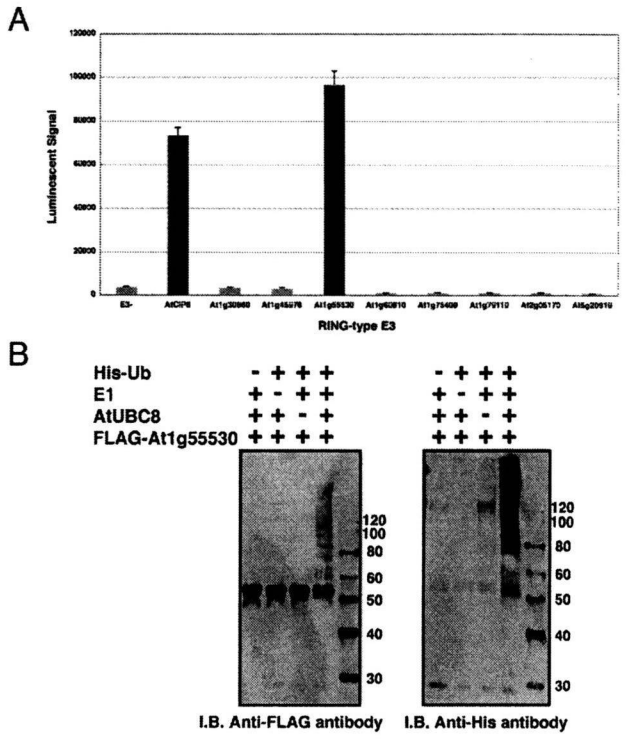

Figure 4
Screening of RING-type E3 ligases having polyubiquitination activity. A, Polyubiquitination reaction of crude recombinant E3 proteins was carried out with mixture of FLAG-tagged and biotinylated ubiquitins, and investigated by luminescent analysis with anti-FLAG antibody. B, Polyubiquitination activity of At1g55530 was confirmed by immunoblot analysis. The assay was carried out using purified recombinant AtUBC8 and At1g55530, and mobility shift of FLAG-tagged At1g55530 and polymer of His-ubiquitin were detected by immunoblot analysis using anti-FLAG and anti-His antibodies, respectively. Error bars represent standard deviations from three independent experiments.

Analysis of the Wheat Cell-free Based Ubiquitination in the Presence of Proteasome Inhibitor

It is known that some cell extracts, such as rabbit reticulocyte or HeLa S-100 fraction, have 26S proteasome-dependent proteolytic activity [28,29]. Based on the presence of endogenous E1 and E2 ubiquitination and polyubiquitination in the wheat cell-free system, it is expected that the 26S proteasome activity will be very low (Fig. 2, 3 and 4). It was previously reported that the wheat germ extract had little 26S proteasome-dependent protein degradation activity [30]. Thus, we determined whether the wheat cell-free system contains active 26S proteasome. Using the crude recombinant proteins that formed polyubiquitin chains in this study, the polyubiquitination reaction was carried out in presence or absence of MG132, and accrual of the polyubiquitinated recombinant pro-

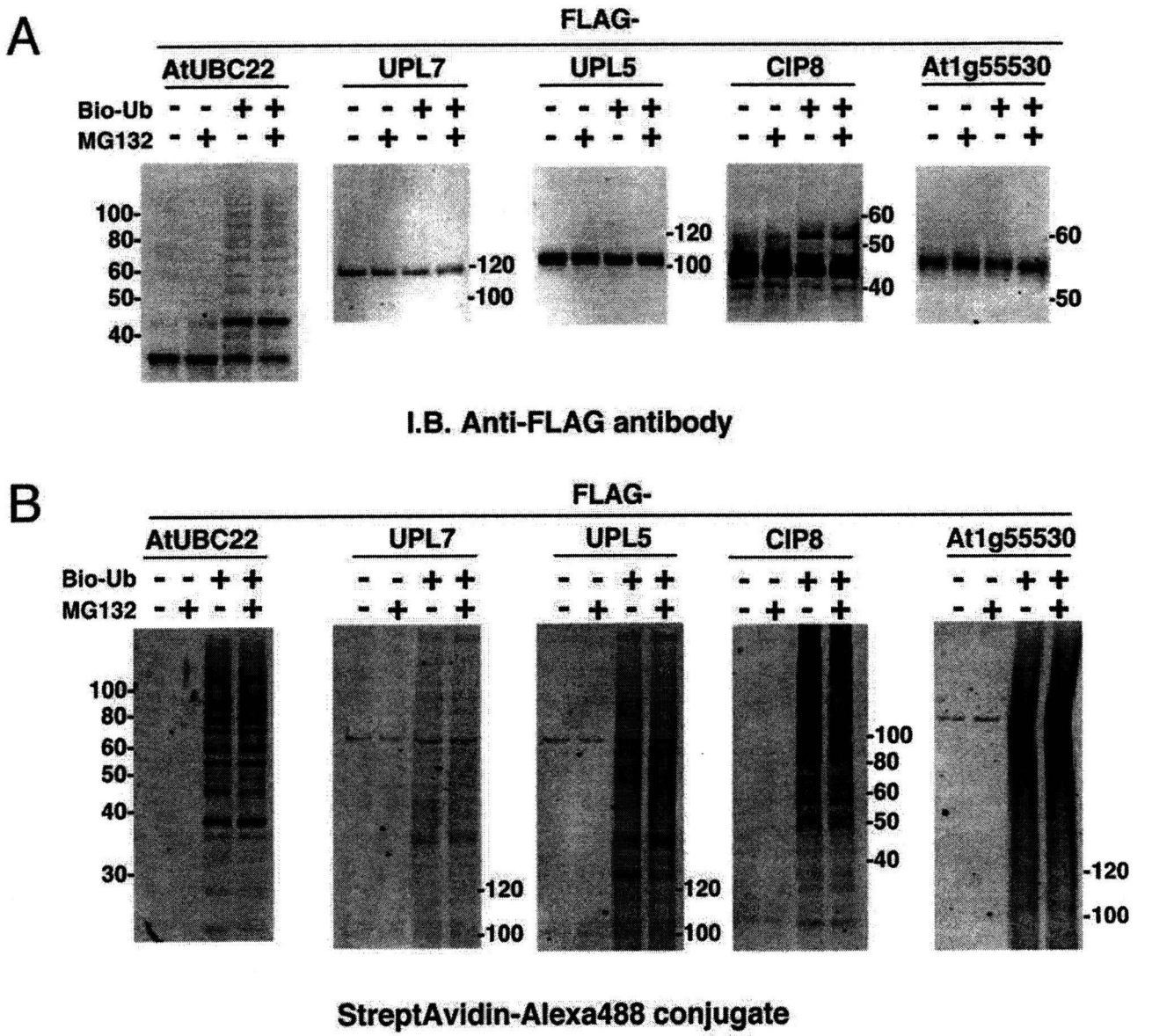

Figure 5
Effect of proteasome inhibitor on stability of polyubiquitinated proteins. Polyubiquitination assays of crude FLAG-tagged E2s and E3s were carried out in the presence or absence of biotinylated ubiquitin and 20 μM MG132. A, FLAG-tagged recombinant proteins were detected by immunoblot analysis using anti-FLAG antibody. B, Polyubiquitination chain formed by each recombinant protein was detected by Alexa488-conjugated streptavidin.

teins and its polyubiquitin chain was estimated. As shown in Fig 5, the amounts of UBC22, UPL5, UPL7 and At1g55530 (Fig. 5A) and of its polyubiquitin chains (Fig. 5B) were hardly altered by MG132 treatment. This result indicates that the proteolytic activity of the 26S proteasome in the wheat cell-free system was below the detection level. Thus, the wheat cell-free system could be suitable for ubiquitination analysis.

Discussion

The ubiquitin signal is an important protein modification in eukaryotes. Binding of a single ubiquitin to a target protein, mono-ubiquitination, is essential for membrane trafficking, protein functions and protein-protein interaction [7]. As for polyubiquitination, both Lys-48- and Lys-63-linked polyubiquitin chains have been well characterized in mammals and yeast. Lys-48 linked chains cause proteolysis of target proteins [6], and Lys-63 linked chains reg-

ulate signal transduction such as cellular localization of protein or protein-protein interactions [7]. In mammals, the multi-functional activities of NF-κB are regulated by the Lys-63 linked chain [31]. In plants, the function of the Lys-63 linked chain is still obscure. However, Arabidopsis E2 and its variants promote formation of the Lys-63 linked chain [32], suggesting that the Lys-63 linked chain in plant cells might also function similar to animal cells. Hence, comprehensive analysis of the ubiquitin-related plant proteins would open a door for elucidation of the plant ubiquitin pathway. In this study, we developed a simple and highly sensitive ubiquitination assay method by combination of the wheat cell-free protein synthesis system and luminescent detection. In general, *in vivo* protein production requires many time-consuming steps such as vector construction, cell culture and purification to obtain the recombinant protein. In contrast, this cell-free based luminescence method could analyze a large amount of ubiquitin reactions without these steps.

Using this method, we conveniently detected polyubiquitin chain formation of E2 and E3s by using two tagged ubiquitins (Fig. 1, 2, 3 and 4). The result of polyubiquitination analysis of the E2s obtained from luminescent-based detection method was verified by immunoblot analysis (Fig. 1). Our analysis also produced recombinant protein of HECT-type E3 ligases without truncation and detected their ubiquitin-conjugation and polyubiquitination activity by luminescent analysis (Fig. 2C and 2D). The ubiquitin-conjugation of UPL5 was not observed when a reductant was added to the reaction (data not shown), suggesting that UPL5 formed a thioester bond with ubiquitin. In addition, the model RING-type E3 CIP8 possessed high polyubiquitin formation activity without substrate, consistent with what was reported previously [26]. Crude recombinant CIP8 formed polyubiquitin chains in the absence of exogenous E1 and E2 (Fig. 3C and 3D), suggesting that the wheat cell-free system might include enough endogenous E1 and E2 activity. It was reported that wheat germ extracts have only a partial ubiquitin pathway [30]. Although the process to isolate wheat germ extract is different from the conventional methods [33], this report strongly supports the existence of endogenous ubiquitin pathway in our wheat cell-free system. Indeed, luminescent analysis using crude recombinant protein showed slight polyubiquitin chain formation even in absence of recombinant E3 (Fig. 2D, Fig. 3C and Fig. 4A, "E3-" lane), indicating that wheat cell-free system might include not only E1 and E2, but E3s or other factors that accelerates the polyubiquitin chain formation. Further, quantitative immunoblot analysis using anti-ubiquitin antibody showed that free ubiquitin was also present in wheat germ extract at a concentration of at least 10 nM (data not shown). This is similar to the ubiquitin concentration supplied in the *in vitro* assay. Although we developed a convenient screening method to detect E3 activity in this study, removal of the endogenous ubiquitin and ubiquitin related components such as E1, E2 and E3, would yield a more sensitive assay. However, wheat cell-free system does not have 26S proteasome proteolytic activity (Fig. 5), indicating that using crude recombinant protein is sufficient for *in vitro* ubiquitination assays.

By using this method, we found that a previously uncharacterized RING type E3, At1g55530, possessed high polyubiquitination activity without exogenous E1 and E2 proteins (Fig. 4). This result suggested that the method developed here is expected to find the activity of other unknown E3 ligases such as At1g55530. Despite having only 32% sequence similarity, the E3s CIP8 and At1g55530 showed similar biochemical functions. Polyubiquitin chains formed by CIP8 and At1g55530 elongated on themselves, while another report showed that polyubiquitin chains were formed on E2 before transferring them to substrates [34]. This reflects that the pattern of polyubiquitin chain formation differs between individual E3s and that the detailed mechanisms are still unknown. These studies suggest the importance of functional analysis using active recombinant proteins. Although we developed a simple screen using crude recombinant E3s in absence of exogenous E1 and E2 (Fig. 4), this method could not detect the activity of some E3 ligases that were unable to utilize endogenous ubiquitination components in wheat cell-free system. The polyubiquitination activity of At5g20910 recombinant protein, expressed in *E. coli* in the presence of AtUBC8 [25], was not active in our *in vitro* system (Fig. 4A), suggesting that in some cases exogenous E2 and/or other components are necessary additions. Such modifications to the ubiquitination assays detailed here would help elucidate the biochemical features of E3s (e.g., addition of recombinant E2s to reaction mixture could give us further information about the E2–E3 specificity, and of other E3 components would lead to the elucidation of structure of complex type E3 ligase such as SCF).

Conclusion

In this study, we found that the wheat cell-free system was an excellent expression system to produce recombinant protein efficiently and to carry out *in vitro* ubiquitination assays without the interference of proteolytic activity. Coupled with luminescent analysis, detection of these ubiquitin reactions in the crude translation reaction mixture was possible. Thus, this method should be helpful for solving the complicated ubiquitin pathway in plant.

Methods

Construction of DNA Templates for Transcription

We used RAFL as templates. DNA templates of E2s and E3s for transcription were constructed by "Split-Primer"

PCR as described previously [17]. Primers used in this study are summarized in Additional file 1. The first round of PCR was performed on each cDNA template using 10 nM of each of the following primers: a target protein specific primer (5'-CCACCCACCACCACCAatgnnnnnnnnn nnnnnnnn-3'; lowercase indicates the 5'-coding region of the target gene) and the AODA2306 primer. Then, a second round of PCR was carried out to construct the templates for protein synthesis using a portion (5 μl) of the first PCR mix, 100 nM SPu primer, 100 nM AODA2303 primer and 1 nM deSP6E02 primer. GST tags were used according to the methods we described previously [17]. The transcription templates of two HECT-type E3 ligases, UPL7 and UPL5, were generated as C-terminal FLAG-tagged proteins using the Gateway System® (Invitrogen, Carlsbad, CA, USA). Briefly, the ORF sequences of UPL7 and UPL5 were amplified by PCR with sense and antisense primers containing attB1 and FLAG-attB2 sequences, respectively. According to the manufacturer's instructions (Invitrogen), these DNA fragments were subcloned into pDONR221 vector by BP reaction and then inserted into the Gateway-based pEU vector (pEU-E01-GW) by LR reaction. Using these recombinant vectors as templates, PCR was carried out with 100 nM SPu primer and 100 nM AODA2303 primer and used as transcription templates.

Cell-free Protein Synthesis

In vitro transcription and cell-free protein synthesis were performed as described [18]. Transcript was made from each of the DNA templates mentioned above using the SP6 RNA polymerase. The synthetic mRNAs were then precipitated with ethanol and collected by centrifugation using a Hitachi R10H rotor. Each mRNA (usually 30–35 μg) was washed and transferred into a translation mixture. The translation reaction was performed in the bilayer mode [35] with slight modifications. The translation mixture that formed the bottom layer consisted of 60 A260 units of the wheat germ extract (CellFree Sciences, Yokohama, Japan) and 2 μg creatine kinase (Roche Diagnostics K. K., Tokyo, Japan) in 25 μl of SUB-AMIX® (CellFree Sciences). The SUB-AMIX® contained (final concentrations) 30 mM Hepes/KOH at pH 8.0, 1.2 mM ATP, 0.25 mM GTP, 16 mM creatine phosphate, 4 mM DTT, 0.4 mM spermidine, 0.3 mM each of the 20 amino acids, 2.7 mM magnesium acetate, and 100 mM potassium acetate. SUB-AMIX® (125 μl) was placed on the top of the translation mixture, forming the upper layer. After incubation at 16°C for 15 h, the synthesized proteins were confirmed by SDS-PAGE. For biotin labeling, 1 μl of crude biotin ligase (BirA) produced by the wheat cell-free expression system was added to the bottom layer, and 0.5 μM (final concentration) of D-biotin (Nacalai Tesque, Inc., Kyoto, Japan) was added to both upper and bottom layers, as described previously [22].

Purification of E2 and E3 Proteins

Purification of GST-tagged protein was carried out according to the procedure described previously [36] with slight modification. Crude GST-tagged recombinant protein (450 μl) produced by the cell-free reaction was precipitated with glutathione sepharose™ 4B (GE Healthcare, Buckinghamshire, UK). The recombinant proteins were eluted with PBS buffer containing 0.1 U of AcTEV protease (Invitrogen) in order to cleave the GST tag from the protein.

Detection of Polyubiquitination by the Luminescent Method

In vitro polyubiquitination assays were carried out in a total volume of 15 μl consisting of 20 mM Tris-HCl pH 7.5, 0.2 mM DTT, 5 mM $MgCl_2$, (10 μM zinc acetate in the assays for RING-type E3s only), 3 mM ATP, 1 mg/ml BSA, 25 nM biotinylated ubiquitin, 25 nM FLAG-tagged ubiquitin, 1 μl of recombinant E2 (purified or crude) and 1 μl of recombinant E3 (purified or crude) in the presence or absence of 0.05 μM rabbit E1 (Boston Biochem, Cambridge, MA, USA) at 30°C for 1 hr in a 384-well Optiplate (PerkinElmer, Boston, MA, USA). In accordance with the AlphaScreen IgG (ProteinA) detection kit (Perkin Elmer) instruction manual, 10 μl of detection mixture containing 20 mM Tris-HCl pH 7.5, 0.2 mM DTT, 5 mM $MgCl_2$, 5 μg/ml Anti-FLAG antibody (Sigma-Aldrich, St. Louis, MO, USA), 1 mg/ml BSA, 0.1 μl streptavidin-coated donor beads and 0.1 μl anti-IgG acceptor beads were added to each well of the 384 Optiplate followed by incubation at 23°C for 1 hr. Luminescence was analyzed by the AlphaScreen detection program.

Detection of Ubiquitinated E2 by Immunoblot Analysis

Crude biotinylated recombinant E2 proteins (40 μl) were used for the ubiquitin-conjugating assay in a total reaction volume of 50 μl containing 20 mM Tris-HCl pH 7.5, 0.2 mM DTT, 5 mM $MgCl_2$, 3 mM ATP and 4 μM FLAG-tagged ubiquitin (Sigma) for 3 hr at 30°C. The reaction products were purified by Streptavidin Magnesphere Paramagnetics particles (Promega, Madison, WI, USA). After washing the beads with PBS buffer, recombinant E2s were boiled in 15 μl of SDS sample buffer containing 50 mM Tris-HCl pH 6.8, 2% SDS, 10% glycerol and 0.2% bromophenol blue, and then separated from the magnet beads. The proteins were separated by SDS-PAGE and transferred to PVDF membrane (Millipore Bedford, MA, USA) according to standard procedures. The blots were detected by the ECL plus detection system (GE Healthcare) with anti-FLAG antibody (Sigma) according to the manufacturer's procedure.

Detection of Polyubiquitination by the Immunoblot Analysis

For polyubiquitination of HECT-type E3 ligases, crude FLAG-tagged UPL recombinant protein (20 μl) was ubiq-

uitinated in a total reaction volume of 50 μl consisting of 20 mM Tris-HCl pH 7.5, 0.2 mM DTT, 5 mM $MgCl_2$, 3 mM ATP, 4 μM biotinylated ubiquitin and 20 μl of crude recombinant AtUBC8 for 3 hr at 30°C. Then, recombinant UPL protein was gathered by anti-FLAG M2 agarose (Sigma). After washing the agarose with PBS buffer, the recombinant UPL protein was boiled in 15 μl of SDS sample buffer and then separated from beads by centrifugation. For polyubiquitination of RING-type E3 ligases, the assay was carried out in 10 μl of reaction mixture containing 20 mM Tris-HCl pH 7.5, 0.2 mM DTT, 5 mM $MgCl_2$, 10 μM zinc acetate, 3 mM ATP, 1 mg/ml BSA, 4 μM FLAG- or His-tagged ubiquitin, 1 μl of purified or crude recombinant E2 and 1 μl of purified or crude recombinant E3 at 30°C for 3 hr. Then, 5 μl of three-fold concentrated SDS sample buffer was added to the reaction mixture and boiled for 5 min. Proteins were separated by SDS-PAGE and transferred to Hybond-LFP PVDF membrane (GE Healthcare) according to standard procedures. Immunoblot analysis was carried out with anti-FLAG antibody (Sigma) or anti-His antibody (GE Healthcare) according to the procedure described above. When detecting biotinylated ubiquitin, blots were treated with 5 μg/ml Alexa488-conjugated streptavidin (Invitrogen) in PBS buffer. After washing with PBS containing 0.1% Tween-20, the blot was analyzed by a Typhoon Imager (GE Healthcare) using the 532 nm laser and 526 emission filters.

Polyubiquitination Assay with 26S Proteasome Inhibitor

Polyubiquitination reaction was carried out as same procedure described above except addition of MG132 (Calbiochem, San Diego, CA, USA) at a final concentration of 20 μM to reaction mixture. Then, the protein on blot was detected by immunoblot analysis with anti-FLAG antibody or Alexa488-conjugated streptavidin.

Authors' contributions

HT conceived the study and performed the experiments, and contributed to writing the manuscript. MS and KS provided RAFL cDNA clones. AN conceived the study. YE conceived the study and supervised the work. TS conceived and designed the study, supervised the work and contributed to writing the manuscript.

Additional material

Additional file 1

AGI code of Arabidopsis genes and primer sequences used in this study.

AGI code of Arabidopsis genes and primer sequences used in this study. Click here for file [http://www.biomedcentral.com/content/supplementary/1471-2229-9-39-S1.xls]

Acknowledgements

This work was partially supported by the Special Coordination Funds for Promoting Science and Technology by the Ministry of Education, Culture, Sports, Science and Technology, Japan (T. S. and Y. E.). We thank Michael Andy Goren for proofreading this manuscript.

References

1. Bai C, Sen P, Hofmann K, Ma L, Goebl M, Harper JW, Elledge SJ: **SKP1 Connects Cell Cycle Regulators to the Ubiquitin Proteolysis Machinery through a Novel Motif, the F-Box.** *Cell* 1996, **86(2)**:263-274.
2. Chen Z, Hagler J, Palombella VJ, Melandri F, Scherer D, Ballard D, Maniatis T: **Signal-induced site-specific phosphorylation targets IκBα to the ubiquitin-proteasome pathway.** *Genes Dev* 1995, **9(13)**:1586-1597.
3. Pickart CM: **Mechanisms underlying ubiquitination.** *Annu Rev Biochem* 2001, **70**:503-533.
4. Smalle J, Vierstra RD: **The ubiquitin 26S proteasome proteolytic pathway.** *Annu Rev Plant Biol* 2004, **55**:555-590.
5. Borden KL: **RING domains: master builders of molecular scaffolds?** *J Mol Biol* 2000, **295(5)**:1103-1112.
6. Glickman MH, Ciechanover A: **The ubiquitin-proteasome proteolytic pathway: destruction for the sake of construction.** *Physiol Rev* 2002, **82(2)**:373-428.
7. Schnell JD, Hicke L: **Non-traditional functions of ubiquitin and ubiquitin-binding proteins.** *J Biol Chem* 2003, **278(38)**:35857-35860.
8. Hofmann RM, Pickart CM: **Noncanonical MMS2-encoded ubiquitin-conjugating enzyme functions in assembly of novel polyubiquitin chains for DNA repair.** *Cell* 1999, **96(5)**:645-653.
9. Yin XJ, Volk S, Ljung K, Mehlmer N, Dolezal K, Ditengou F, Hanano S, Davis SJ, Schmelzer E, Sandberg G, Teige M, Palme K, Pickart C, Bachmair A: **Ubiquitin lysine 63 chain forming ligases regulate apical dominance in Arabidopsis.** *Plant Cell* 2007, **19(6)**:1898-1911.
10. Hicke L: **A new ticket for entry into budding vesicles – ubiquitin.** *Cell* 2001, **106(5)**:527-530.
11. Vierstra RD: **The ubiquitin/26S proteasome pathway, the complex last chapter in the life of many plant proteins.** *Trends Plant Sci* 2003, **8(3)**:135-142.
12. Nelson DC, Lasswell J, Rogg LE, Cohen MA, Bartel B: **FKF1, a Clock-Controlled Gene that Regulates the Transition to Flowering in Arabidopsis.** *Cell* 2000, **101(3)**:331-340.
13. Osterlund MT, Hardtke CS, Wei N, Deng XW: **Targeted destabilization of HY5 during light-regulated development of Arabidopsis.** *Nature* 2000, **405(6785)**:462-466.
14. Stone SL, Williams LA, Farmer LM, Vierstra RD, Callis J: **KEEP ON GOING, a RING E3 ligase essential for Arabidopsis growth and development, is involved in abscisic acid signaling.** *Plant Cell* 2006, **18(12)**:3415-3428.
15. Rosebrock TR, Zeng L, Brady JJ, Abramovitch RB, Xiao F, Martin GB: **A bacterial E3 ubiquitin ligase targets a host protein kinase to disrupt plant immunity.** *Nature* 2007, **448(7151)**:370-374.
16. Kraft E, Stone SL, Ma L, Su N, Gao Y, Lau OS, Deng XW, Callis J: **Genome analysis and functional characterization of the E2 and RING-type E3 ligase ubiquitination enzymes of Arabidopsis.** *Plant Physiol* 2005, **139(4)**:1597-1611.
17. Sawasaki T, Ogasawara T, Morishita R, Endo Y: **A cell-free protein synthesis system for high-throughput proteomics.** *Proc Natl Acad Sci USA* 2002, **99(23)**:14652-14657.
18. Sawasaki T, Gouda MD, Kawasaki T, Tsuboi T, Tozawa Y, Takai K, Endo Y: **The wheat germ cell-free expression system: methods for high-throughput materialization of genetic information.** *Methods Mol Biol* 2005, **310**:131-144.
19. Kobayashi T, Kodani Y, Nozawa A, Endo Y, Sawasaki T: **DNA-binding profiling of human hormone nuclear receptors via fluorescence correlation spectroscopy in a cell-free system.** *FEBS Lett* 2008, **582(18)**:2737-2744.
20. Seki M, Narusaka M, Kamiya A, Ishida J, Satou M, Sakurai T, Nakajima M, Enju A, Akiyama K, Oono Y, Muramatsu M, Hayashizaki Y, Kawai J, Carninci P, Itoh M, Ishii Y, Arakawa T, Shibata K, Shinagawa A, Shinozaki K: **Functional annotation of a full-length Arabidopsis cDNA collection.** *Science* 2002, **296(5565)**:141-145.
21. Kus B, Gajadhar A, Stanger K, Cho R, Sun W, Rouleau N, Lee T, Chan D, Wolting C, Edwards A, Bosse R, Rotin D: **A high throughput**

screen to identify substrates for the ubiquitin ligase Rsp5. *J Biol Chem* 2005, **280(33)**:29470-29478.
22. Sawasaki T, Kamura N, Matsunaga S, Saeki M, Tsuchimochi M, Morishita R, Endo Y: **Arabidopsis HY5 protein functions as a DNA-binding tag for purification and functional immobilization of proteins on agarose/DNA microplate.** *FEBS Lett* 2008, **582(2)**:221-228.
23. Bates PW, Vierstra RD: **UPL1 and 2, two 405 kDa ubiquitin-protein ligases from Arabidopsis thaliana related to the HECT-domain protein family.** *Plant J* 1999, **20(2)**:183-195.
24. Downes BP, Stupar RM, Gingerich DJ, Vierstra RD: **The HECT ubiquitin-protein ligase (UPL) family in Arabidopsis: UPL3 has a specific role in trichome development.** *Plant J* 2003, **35(6)**:729-742.
25. Stone SL, Hauksdóttir H, Troy A, Herschleb J, Kraft E, Callis J: **Functional analysis of the RING-type ubiquitin ligase family of Arabidopsis.** *Plant Physiol* 2005, **137(1)**:13-30.
26. Hardtke CS, Okamoto H, Deng XW: **Biochemical evidence for ubiquitin ligase activity of the Arabidopsis COP1 interacting protein 8 (CIP8).** *Plant J* 2002, **30(4)**:385-394.
27. Yamauchi K, Wada K, Tanji K, Tanaka M, Kamitani T: **Ubiquitination of E3 ubiquitin ligase TRIMa and its potential role.** *FEBS J* 2008, **275(7)**:1540-1555.
28. Waxman L, Fagan JM, Goldberg AL: **Demonstration of two distinct high molecular weight proteases in rabbit reticulocytes, one of which degrades ubiquitin conjugates.** *J Biol Chem* 1987, **262(6)**:2451-2457.
29. Chen ZJ, Parent L, Maniatis T: **Site-Specific Phosphorylation of IκBα by a Novel Ubiquitination-Dependent Protein Kinase Activity.** *Cell* 1996, **84(6)**:853-862.
30. Hatfield PM, Vierstra RD: **Ubiquitin-dependent proteolytic pathway in wheatgerm: Isolation of multiple forms of ubiquitin-activating enzyme, E1.** *Biochemistry* 1989, **28**:735-742.
31. Wu CJ, Conze DB, Li T, Srinivasula SM, Ashwell JD: **Sensing of Lys 63-linked polyubiquitination by NEMO is a key event in NF-κB activation.** *Nature Cell Biol* 2006, **8(4)**:398-406.
32. Yin XJ, Volk S, Ljung K, Mehlmer N, Dolezal K, Ditengou F, Hanano S, Davis SJ, Schmelzer E, Sandberg G, Teige M, Palme K, Pickart C, Bachmaira A: **Ubiquitin lysine 63 chain-forming ligases regulate apical dominance in Arabidopsis.** *Plant Cell* 2007, **19(6)**:1898-1911.
33. Madin K, Sawasaki T, Ogasawara T, Endo Y: **A highly efficient and robust cell-free protein synthesis system prepared from wheat embryos: Plants apparently contain a suicide system directed at ribosomes.** *Proc Natl Acad Sci USA* 2000, **97(2)**:559-564.
34. Li W, Tu D, Brunger AT, Ye Y: **A ubiquitin ligase transfers preformed polyubiquitin chains from a conjugating enzyme to a substrate.** *Nature* 2007, **446(7133)**:333-337.
35. Sawasaki T, Hasegawa Y, Tsuchimochi M, Kamura N, Ogasawara T, Kuroita T, Endo Y: **A bilayer cell-free protein synthesis system for high-throughput screening of gene products.** *FEBS Lett* 2002, **514(1)**:102-105.
36. Masaoka T, Nishi M, Ryo A, Endo Y, Sawasaki T: **The wheat germ cell-free based screening of protein substrates of calcium/calmodulin-dependent protein kinase II delta.** *FEBS Lett* 2008, **582(13)**:1795-1801.

FEBS Letters 583 (2009) 1243–1250

ELSEVIER

FEBS Letters

journal homepage: www.FEBSLetters.org

Requirement for microtubule integrity in the SOCS1-mediated intracellular dynamics of HIV-1 Gag

Mayuko Nishi [a,b], Akihide Ryo [a,b,*], Naomi Tsurutani [c], Kenji Ohba [a], Tatsuya Sawasaki [d], Ryo Morishita [d], Kilian Perrem [e], Ichiro Aoki [b], Yuko Morikawa [c], Naoki Yamamoto [a,*]

[a] AIDS Research Center, National Institute of Infectious Diseases, 1-23-1 Toyama, Shinjuku-ku, Tokyo, Japan 162-8640, Japan
[b] Department of Pathology, Yokohama City University School of Medicine, 3-9 Fuku-ura, Kanazawa-ku, Yokohama 236-0004, Japan
[c] Kitasato Institute for Life Sciences, Kitasato University, Shirokane 5-9-1, Minato-ku, Tokyo 108-8641, Japan
[d] Cell Free Science and Research Center, Ehime University, Ehime 790-8577, Japan
[e] CSIRO, P.O. Box 225, Dickson ACT 2602, Australia

ARTICLE INFO

Article history:
Received 8 December 2008
Revised 16 March 2009
Accepted 18 March 2009
Available online 25 March 2009

Edited by Kaspar Locher

Keywords:
HIV
Host factor
Suppressor of cytokine signaling 1
Microtubule
Ubiquitin
Trafficking

ABSTRACT

Suppressor of cytokine signaling 1 (SOCS1) is a recently identified host factor that positively regulates the intracellular trafficking and stability of HIV-1 Gag. We here examine the molecular mechanism by which SOCS1 regulates intercellular Gag trafficking and virus particle production. We find that SOCS1 colocalizes with Gag along the microtubule network and promotes microtubule stability. SOCS1 also increases the amount of Gag associated with microtubules. Both nocodazole treatment and the expression of the microtubule-destabilizing protein, stathmin, inhibit the enhancement of HIV-1 particle production by SOCS1. SOCS1 facilitates Gag ubiquitination and the co-expression of a dominant-negative ubiquitin significantly inhibits the association of Gag with microtubules. We thus propose that the microtubule network plays a role in SOCS1-mediated HIV-1 Gag transport and virus particle formation.

Structured summary:
MINT-7014185: *Gag* (uniprotkb:P05888) and *SOCS1* (uniprotkb:O15524) *colocalize* (MI:0403) by *cosedimentation* (MI:0027)
MINT-7014239: *Cullin 2* (uniprotkb:Q13617) *physically interacts* (MI:0218) with *RelA* (uniprotkb:Q04206), *RBX1* (uniprotkb:P62877), *SOCS1* (uniprotkb:O15524), *elongin B* (uniprotkb:Q15369) and *elongin C* (uniprotkb:Q15370) by *pull-down* (MI:0096)
MINT-7014046: *gag* (uniprotkb:P05888), *SOCS1* (uniprotkb:O15524) and *tubulin alpha* (uniprotkb:Q13748) *colocalize* (MI:0403) by *fluorescence microscopy* (MI:0416)
MINT-7014269: *tubulin alpha* (uniprotkb:Q13748) *physically interacts* (MI:0218) with *Gag* (uniprotkb:P05888) by *anti tag coimmunoprecipitation* (MI:0007)
MINT-7014036: *tubulin alpha* (uniprotkb:Q13748) and *SOCS1* (uniprotkb:O15524) *colocalize* (MI:0403) by *fluorescence microscopy* (MI:0416)
MINT-7014201: *Cullin 2* (uniprotkb:Q13617) *physically interacts* (MI:0218) with *RBX1* (uniprotkb:P62877), *SOCS1* (uniprotkb:O15524), *elongin B* (uniprotkb:Q15369) and *elongin C* (uniprotkb:Q15370) by *pull-down* (MI:0096)
MINT-7014257: *Gag* (uniprotkb:P05888) *physically interacts* (MI:0218) with *Ubiquitin* (uniprotkb:P62988) by *anti tag coimmunoprecipitation* (MI:0007)
MINT-7014221: *Cullin 2* (uniprotkb:Q13617) *physically interacts* (MI:0218) with *Gag* (uniprotkb:P05888), *elongin C* (uniprotkb:Q15370), *elongin B* (uniprotkb:Q15369), *SOCS1* (uniprotkb:O15524) and *RBX1* (uniprotkb:P62877) by *pull-down* (MI:0096)

1. Introduction

The human immunodeficiency virus 1 (HIV-1) employs multistep and multi-factorial processes for producing progeny viruses during infection [1,2]. Virus must utilize the intrinsic transport machinery of the infected host cells to enable the active transport

Abbreviations: HIV, human immunodeficiency virus; SOCS1, Suppressor of cytokine signaling 1; KIR, kinase inhibitory region; MTOC, microtubule organizing center; Ub, ubiquitin; VLP, virus-like particle

* Corresponding authors. Address: AIDS Research Center, National Institute of Infectious Diseases, 4-7-1 Gakuen, Musashimurayama, Tokyo 208-0011, Japan (A. Ryo). Fax: +81 42 563 6291.
E-mail addresses: aryo@nih.go.jp (A. Ryo), nyama@nih.go.jp (N. Yamamoto).

0014-5793/$36.00 © 2009 Federation of European Biochemical Societies. Published by Elsevier B.V. All rights reserved.
doi:10.1016/j.febslet.2009.03.041

of viral proteins [3,4]. Several recent studies have identified cellular factors that modulate HIV-1 Gag trafficking and localization. These include AP-3δ, POSH, HP68, GGA and Trim22 [5–9]. Moreover, phosphatidylinositol-(4,5)-bisphosphate (PIP2) has been shown to control the targeting of Gag to the plasma membrane [10]. These findings point to a critical role of host cell factors in Gag assembly and release, but the precise molecular functions of these factors and the specific timing of their roles in this process remain largely unknown.

We recently reported that the suppressor of cytokine signaling 1 (SOCS1) is an inducible host factor during HIV-1 infection and plays an important role in the intracellular trafficking of Gag to the plasma membrane, resulting in the efficient production of HIV-1 particles [11]. Moreover, we have further shown that the function of SOCS1 in Gag trafficking and HIV-1 particle production is not principally due to the suppression of interferon/cytokine signaling, but is mediated via its interaction with the HIV-1 Gag polyprotein [11]. Importantly, the targeted depletion of SOCS1 results in the mistargeting and degradation of Gag in lysosomes, leading to a significant decrease in virus particle production [11].

In our current study, we have utilized SOCS1 as a molecular tool to further reveal the molecular mechanisms underlying the intracellular transport of HIV-1 Gag during viral infection. We reveal from our findings that SOCS1 regulates the Gag trafficking process via the microtubule-dependent cellular machinery. Furthermore, we find that Gag is also regulated by a ubiquitin signaling pathway which is accompanied by Gag ubiquitination. These findings shed new light on the mechanisms involved in the intracellular transport of HIV-1 Gag and provide important clues for the design of future novel therapeutic interventions against AIDS and related disorders.

2. Materials and methods

2.1. Antibodies

Antibodies (Abs) and fluorescent reagents were obtained from the following sources: rabbit polyclonal anti-myc (A-14) and rabbit polyclonal anti-SOCS1 (H-93) Abs (Santa Cruz Biotechnology); rabbit polyclonal anti-SOCS1 (Zymed Laboratories); mouse monoclonal anti-FLAG (M2), anti-α-tubulin, anti-acetylated-α-tubulin and anti-γ-tubulin Abs (Sigma, St. Louis, MO); rabbit polyclonal anti-stathmin antibody (Calbiochem); mouse monoclonal anti-myc antibody (9B11, Cell Signaling Technology); mouse monoclonal anti-cytokeratin 7, cytokeratin 18, vimentin and HIV-p24 Ab (Dako Cytomation). Immunoblotting, immunoprecipitation and immunofluorescent analyses were performed as described previously [11].

2.2. Plasmids and sequences

Expression constructs for SOCS1 have been described previously [12]. HIV-1 Gag constructs have also been described previously [13]. Stathmin cDNA was amplified by RT-PCR from a human kidney cDNA library using the primers 5′-AGCAAG CTTGCCACCATGGCTTCTTCTGATATCCAGG-3′ and 5′-GACGGATCC GTCAGCTTCAGTCTCGTCAG-3′ and then subcloned into the pcDNA3.1 vector. pcDNA3.1-myc-ubiquitin and its mutants were generated by PCR as described previously [14]. The siRNA sequences were as follows: SOCS1-siRNA, GGCCAGAACCTT CCTCCTCTT; control-siRNA, TCGTATGTTGTGTGGAATT. All expression constructs were validated by sequencing.

2.3. Microtubule-associated protein spin-down assays

Microtubule-associated proteins were collected using a microtubule-associated protein spin-down assay kit (Cytoskeleton, BK029) according to the manufacturer's instructions. Briefly, 293T cells were lysed in 0.5 ml of PEM buffer (80 mM PIPES, pH 6.9, 0.3% Triton X-100, 1 mM EGTA, 1 mM GTP, GTP, 1 mM $MgCl_2$) supplemented with 1 mM phenylmethylsulfonyl fluoride, 5 μg/ml leupeptin, 2 μg/ml aprotinin, 1 mM sodium orthovanadate, and 5 mM NaF. Cell lysates were incubated with taxol-stabilized microtubules, followed by ultracentrifuge at 100000×g for 40 min at 25 ℃.

2.4. Cell culture

The 293T, COS-1, COS-7, HeLa and HOS cell lines and mouse embryonic fibroblasts (MEFs) were cultured in DMEM supplemented with 10% FBS. SOCS1−/− MEF cells were cultured as described previously [12].

2.5. In vitro interaction analysis

The in vitro interaction between HIV-1 Gag and the SOCS1-E3 complex was analyzed as follows: ^{14}C-labeled recombinant proteins (SOCS1, elongin B/C, Rbx1, biotin labeled cullin 2, and HIV-1 Gag) were synthesized in a wheat germ cell-free system as described previously [15]. The synthesized proteins were subsequently incubated in 120 μl of reaction buffer (50 mM Tris–HCl, pH 7.6, 50 mM $MgCl_2$, 500 mM CH_3COOK, 0.1 mM DTT and 1 mg/ml BSA) and streptavidin magnetic beads (Promega, Madison, WI) at 23 °C for 1 h. The precipitated proteins were then washed three times with reaction buffer and subjected to autoradiography.

3. Results

3.1. SOCS1 aligns with microtubule forming fibrous structures

SOCS1 has been shown previously to localize at both the perinuclear region and the microtubule organizing center (MTOC) [16]. This finding indicated the possible involvement of the microtubule network in the regulation of Gag by SOCS1. We thus addressed whether the Gag transport system is in fact mediated by microtubule integrity and if SOCS1 enhances this process. Immunofluorescent analysis with α-tubulin antibodies revealed that endogenous SOCS1 forms punctate structures that align with the microtubule network (Fig. 1A). Importantly, these signals were completely abolished when the cells were stained with anti-SOCS1 antibodies that had been pre-absorbed with recombinant SOCS1 protein, confirming the specificity of this antibody (Fig. 1B). Parallel experiments revealed that SOCS1 does not colocalize with other cytoskeletal components such as actin or intermediate filaments (Fig. 1C).

3.2. SOCS1 promotes microtubule stability

Given our finding that SOCS1 can tightly associate with microtubules, we next addressed whether SOCS1 affects microtubule stability. Stabilized microtubules are frequently enriched in tubulin that has undergone post-translational modifications such as acetylation [17]. We found that the high expression of SOCS1 results in higher amounts of acetylated microtubules in three different cell lines when compared with control cells (Fig. 2A) and that this trend is dose-dependent in COS-7 cells (Fig. 2B). On the other hand, SOCS1−/− mouse embryonic fibroblasts (MEFs) exhibited lower levels of acetylated α-tubulin compared with wild-type MEFs (Fig. 2C). These results indicate that SOCS1 does indeed contribute to the stabilization of microtubules.

Mammalian cells usually possess a population of microtubules that are resistant to the depolymerization effects of microtubule disorganizing reagents. We thus addressed whether SOCS1 impacts

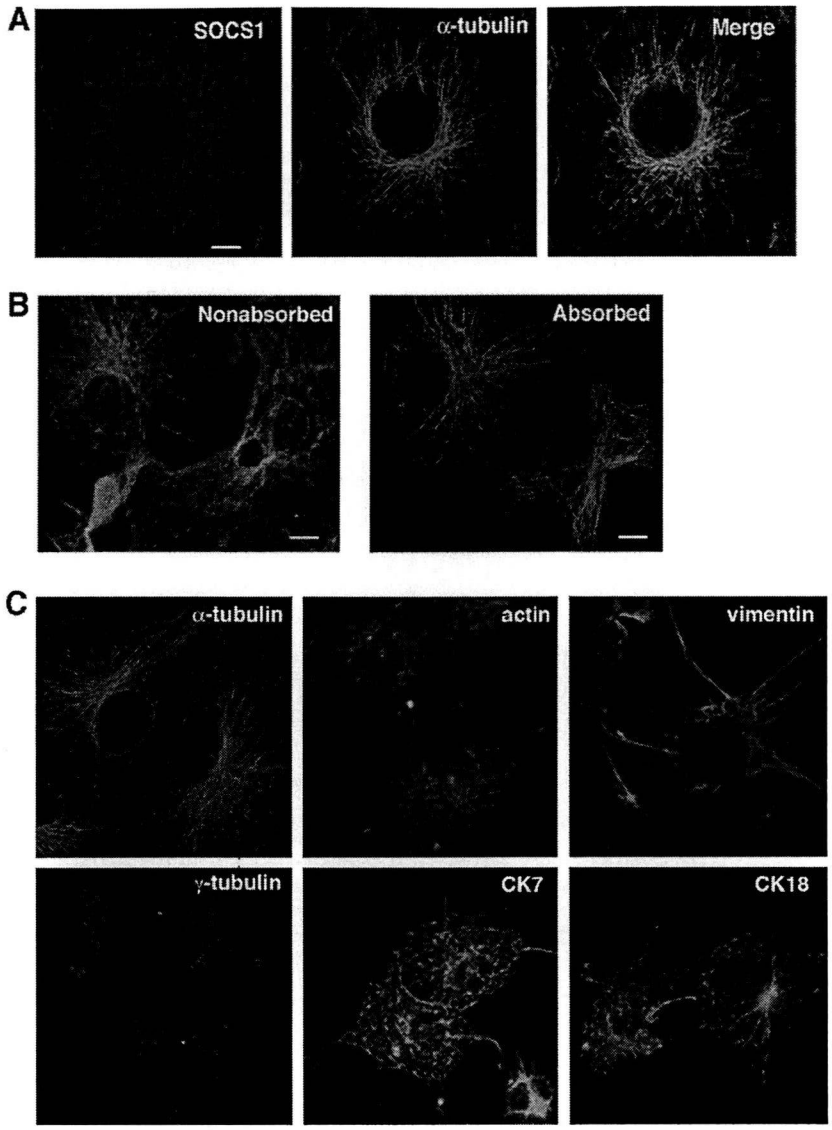

Fig. 1. SOCS1 colocalizes with microtubule forming fibrous structures. (A) COS-1 cells were fixed with 3% formaldehyde followed by 100% cold methanol, and then co-immunostained with polyclonal antibodies targeting SOCS1 (red) and monoclonal antibodies targeting α-tubulin (green). Cells were then analyzed by confocal microscopy. Scale bar, 10 μm. (B) COS-1 cells were immunostained with anti-α-tubulin monoclonal antibodies together with anti-SOCS1 polyclonal antibodies that had either been non-absorbed or pre-absorbed with GST-SOCS1 proteins. This was followed by confocal microscopy. Scale bar, 10 μm. (C) COS-1 cells were fixed with 3% formaldehyde followed by 100% cold methanol, then co-immunostained with polyclonal antibodies targeting SOCS1 (red) and monoclonal antibodies targeting various cytoskeletal components (green). Cells were then analyzed by confocal microscopy.

upon this property in this subpopulation of microtubules in COS-7 cells. The cells were transfected with either SOCS1 or control vector and then treated with 1 μM colchicine for 12 h to fully depolymerize the microtubules. Immunostaining with antibodies against acetylated α-tubulin showed that the SOCS1 expressing cells contained more polymerized microtubules compared with the control cells (Fig. 2D). These results indicate that SOCS1 might contribute to the microtubule stability required for Gag trafficking via this network.

3.3. SOCS1 enhances the association of HIV-1 Gag with microtubules

We next investigated the sub-cellular localization of HIV-1 Gag with SOCS1 and microtubules. COS-1 cells were transfected with Gag-GFP and after 24 h were fixed with 3% formaldehyde, followed by 100% cold methanol. The cells were then immunostained with anti-SOCS1 and anti-α-tubulin antibodies. Consistent with our earlier results, confocal microscopic analysis revealed that SOCS1 can form dotted filamentous structures in the cytoplasm along the microtubules, and that HIV-1 Gag colocalizes with these SOCS1 puncta (Fig. 3A).

To next determine whether cellular SOCS1 and Gag can together mechanically bind microtubules, and thus whether SOCS1 expression has any impact upon the interaction between Gag and microtubules, we performed microtubule pull-down analysis. 293T cells were transfected with either Gag-FLAG, myc-SOCS1, or a combination of these two plasmids, and the lysates from these transfected cells were subsequently incubated with taxol-stabilized microtubules and centrifuged to pellet the microtubule-associated proteins. The pellet fractions were then subjected to immunoblotting using either anti-myc or anti-FLAG antibodies. SOCS1 was found to be co-sedimented with microtubules irrespective of whether Gag had been co-transfected (Fig. 3B). The quantities of microtubule-bound Gag in the pellet fraction, however, were significantly increased when SOCS1 was co-transfected (Fig. 3B). These results together indicate that SOCS1 is itself a microtubule binding protein that may also mediate the interaction between HIV-1 Gag and microtubules.

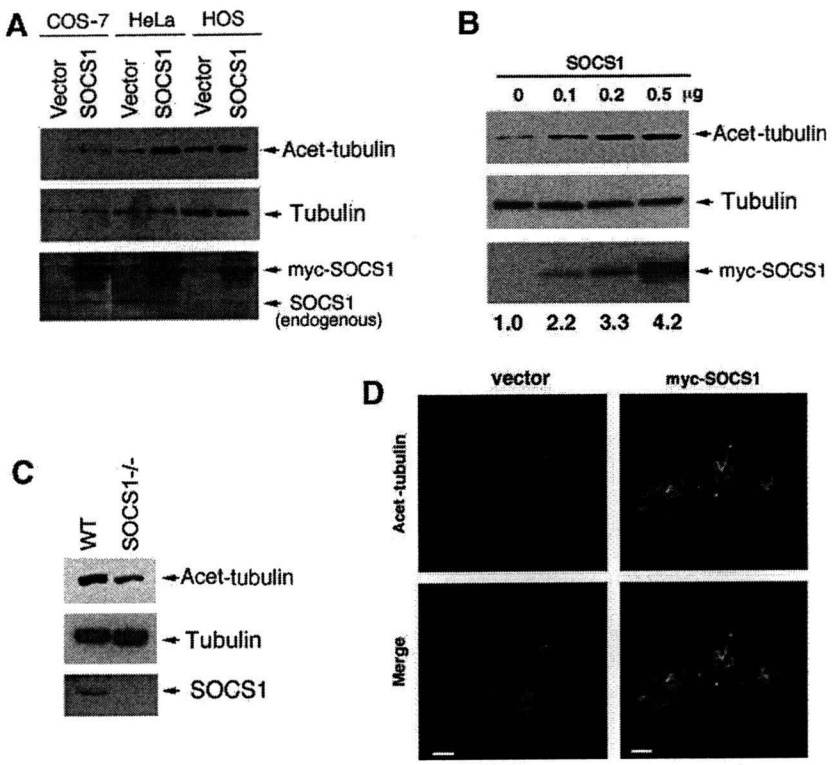

Fig. 2. SOCS1 enhances microtubule stability. (A) COS-7, HeLa or HOS cells were transfected with either empty vector or myc-SOCS1 for 48 h. Cell lysates were then subjected to immunoblotting analysis with antibodies against α-tubulin, acetylated α-tubulin or SOCS1. (B) COS-7 cells were transfected with various amounts of myc-SOCS1 as in (A). Cell lysates were then subjected to immunoblotting analysis with anti-α-tubulin, anti-acetylated-α-tubulin or anti-myc antibodies. Numerical values below the blots indicate acetylated α-tubulin signal intensities normalized by the unmodified α-tubulin intensity derived by densitometry. (C) Exponentially growing wild-type MEFs or SOCS1−/− MEFs were lysed and the cell lysates were immunoblotted with antibodies against α-tubulin, acetylated α -tubulin or SOCS1. (D) COS-7 cells were co-transfected with empty vector or myc-SOCS1, and then treated with colchicine (1 μM) for 12 h to depolymerize the microtubules. Cells were then fixed and immunostained with both anti-acetylated-α-tubulin (green) or anti-myc (red) antibodies and then stained with 4′,6-diamino-2-phenylindole (DAPI, blue), followed by confocal microscopy. Scale bar, 10 μm.

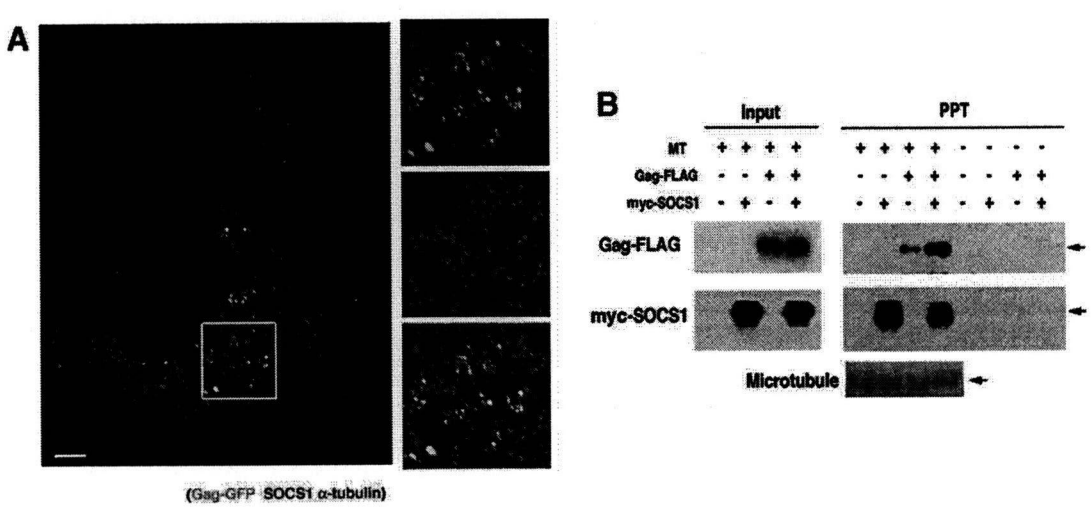

Fig. 3. SOCS1 enhances HIV-1 Gag associated with microtubules. (A) COS-1 cells transiently transfected with HIV-1 Gag-GFP were co-immunostained with antibodies targeting endogenous SOCS1 (red) and microtubules (α-tubulin, blue). The inset indicates the area shown at higher magnification in the right hand panels which reveal the colocalization of Gag-GFP with SOCS1 along the microtubules. Scale bar, 10 μm. (B) Cosedimentation of SOCS1 and HIV-1 Gag with polymerized microtubules. 293T cells were transfected with the indicated plasmids for 36 h. Cell lysates were then incubated with taxol-stabilized microtubules or control buffer and separated into precipitate (PPT) and supernatant fractions. Precipitate fractions were subjected to immunoblotting analysis with anti-myc or anti-FLAG antibodies.

3.4. Microtubule integrity is required for SOCS1 to function in HIV-1 particle formation

Our results shown above indicated that SOCS1 mediates the association of HIV-1 Gag with the microtubule networks. We next examined therefore whether SOCS1-mediated Gag trafficking, and the resultant HIV-1 particle production, are dependent upon an intact microtubule network. 293T cells were transfected with the HIV-1 molecular clone pNL4-3 and co-transfected with either empty vector alone or myc-SOCS1. After 24 h, the cells were washed with PBS and then cultured in the presence or absence of nocodazole for a further 6 h. Subsequent measurement of the p24 antigen levels in the cell supernatant by ELISA revealed nocodazole treatment significantly inhibited the enhancement of HIV-1 particle production in SOCS1-transfected cells more dramatically than in vector control transfected cells, and that this was

dose-dependent (Fig. 4A). Consistent with these results also, SOCS1 localization was observed to be significantly altered by nocodazole treatment, i.e. from a dotted filamentous structure along the microtubules to diffuse and larger aggregations in the cytoplasm (Fig. 4B). The use of trypan blue dye exclusion confirmed that cell viability was not affected by the nocodazole treatment (Fig. 4C).

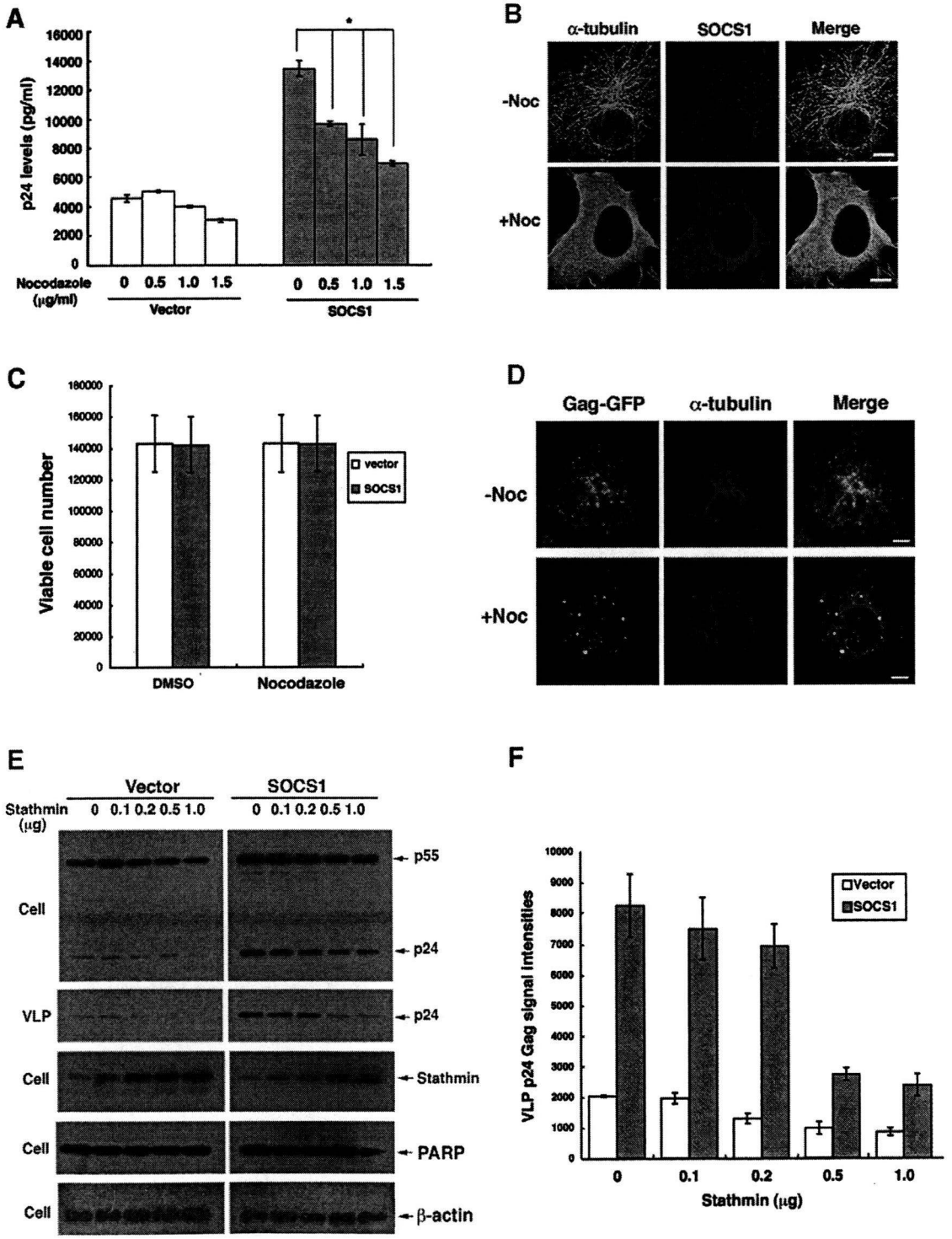

Fig. 4. Microtubule integrity is required for SOCS1 to function in HIV-1 particle formation. (A) 293T cells were transfected with pNL4-3, and co-transfected with either empty vector alone (Vector) or myc-SOCS1. After 24 h, cells were washed with PBS and then cultured with fresh media including the indicated concentrations of nocodazole for 6 h. Supernatant p24 antigen levels were measured by p24 ELISA. The data shown are the average ± S.D. of three independent experiments. $^{*}P \leqslant 0.05$, by the Student's *t*-test. (B and C) Mislocalization of SOCS1 in cells treated with nocodazole. COS-1 cells were treated with vehicle only or with nocodazole (2 μg/ml) for 6 h. Cells were then fixed and immunostained with both anti-SOCS1 (red) and anti-α-tubulin (green) antibodies, followed by confocal microscopy (B). Scale bar, 10 μm. The numbers of viable cells were calculated by trypan blue dye exclusion (C). (D) COS-1 cells transfected with Gag-GFP were treated with vehicle only or with nocodazole (2 μg/ml) for 6 h followed by immunostaining with anti-α-tubulin (red) antibody. Scale bar, 10 μm. (E and F) 293T cells were transfected with pNL4-3 and either vector or SOCS1, and co-transfected with various amounts of stathmin. At 36 h after transfection, cell lysate and supernatant virus-like particle (VLP) were processed for immunoblotting analysis with anti-p24, anti-PARP, anti-β-actin or anti-stathmin antibodies (E). VLP p24 Gag signal intensities, derived by densitometry, are shown in (F).

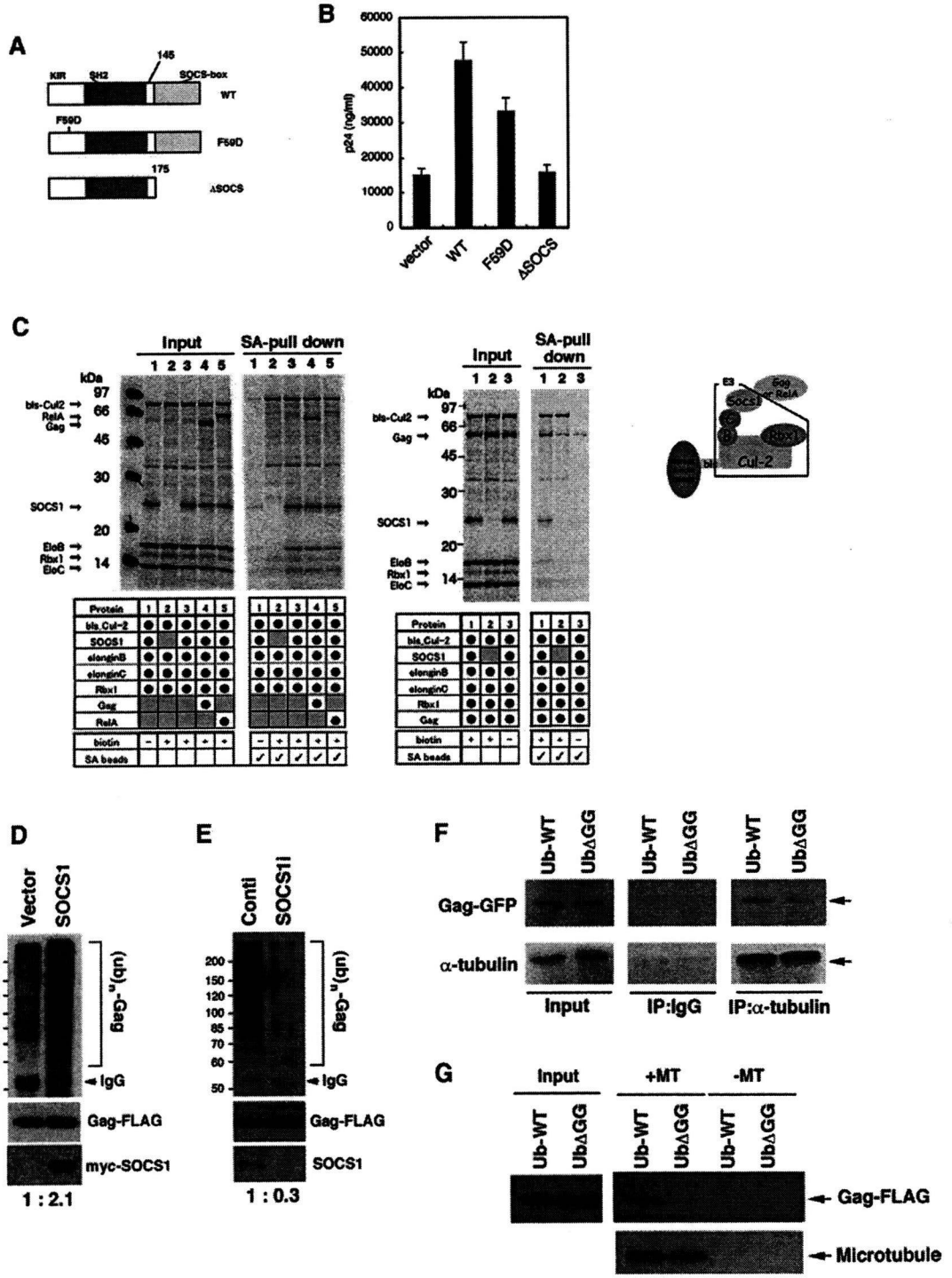

Fig. 5. SOCS1 enhances the ubiquitination of HIV-1 Gag and this affects the association of Gag with the microtubules. (A) Schematic represenation of SOCS1 mutants. (B) 293T cells were transfected with pNL4-3 and co-transfected with control vector, wild-type SOCS1 (WT), SOCS1-F59D mutant or ΔSOCS-box mutant. After 48 h, the p24 levels in the cell supernatants were measured by ELISA. (C) HIV-1 Gag associates with the ubiquitin ligase complex of SOCS1 in vitro. ^{14}C-labeled proteins (SOCS1, biotin labeled Cullin2, elongin B/C, Rbx1, HIV-1 Gag and RelA) were synthesized using a wheat germ cell-free system. Purified proteins were incubated in the indicated combinations for 1 h and subjected to co-purification with streptavidin magnetic beads. Captured proteins were then separated by SDS–PAGE followed by autoradiography. (D) 293T cells were co-transfected with Gag-FLAG, myc-tagged ubiquitin, and either empty vector (Vector) or SOCS1 expression construct. After 48 h, cells were lysed and denatured by boiling them in 1% SDS lysis buffer and diluted to RIPA buffer conditions, and Gag-FLAG proteins were immunoprecipitated (IP) with anti-FLAG antibody and processed for anti-myc immunoblotting to detect ubiquitinated Gag. Ubn, polyubiquitinated. Numerical values below blot indicates the relative levels of ubiquitinated Gag normalized by the amount of total Gag. (E) 293T cells were co-transfected with Gag-FLAG, myc-tagged ubiquitin, and either control-siRNA or SOCS1-siRNA. After 48 h, cell lysates were immunoprecipitated with anti-FLAG antibody and processed for anti-myc immunoblotting to detect ubiquitinated Gag. Ubn, polyubiquitinated. Numerical values below blot indicates the relative levels of ubiquitinated Gag normalized by the amount of total Gag. (F) 293T cells were transfected with Gag-GFP and SOCS1, and co-transfected with either myc-Ub-WT or myc-UbΔGG. After 24 h, cell lysates were harvested and subjected to immunoprecipitation analysis with anti-α-tubulin antibody or non-immunized mouse IgG (IgG) followed by immunoblotting analysis with the indicated antibodies. (G) 293T cells were transfected with Gag-FLAG and SOCS1, and co-transfected with either myc-Ub-WT or myc-UbΔGG. After 24 h, cell lysates were harvested and then incubated with taxol-stabilized microtubules (+MT) or control buffer (−MT), and separated into precipitate and supernatant fractions. Precipitate fractions were collected and then subjected to immunoblotting analysis with either anti-FLAG or anti-α-tubulin (microtubule) antibodies.

Furthermore, a parallel experiment revealed that the Gag-GFP puncta formed larger aggregations in the cytoplasm upon nocodazole treatment (Fig. 4D).

To further delineate the role of microtubule integrity in HIV-1 particle formation, we next performed experiments in which we co-transfected SOCS1 and pNL4-3 with or without the microtubule-destabilizing protein stathmin. Stathmin expression efficiently blocked the effects of SOCS1 upon HIV-1 particle formation in a dose-dependent manner (Fig. 4E and F). Cell viability was not strongly affected as revealed by immunoblotting analysis of either poly (ADP-ribose) polymerase (PARP) or β-actin (Fig. 4E). Our findings together indicate therefore that microtubule integrity may be required for SOCS1 to function in Gag assembly and release.

3.5. SOCS1 facilitates the ubiquitination of HIV-1 Gag

Our previous study has revealed that the SOCS-box of SOCS1 is required for both HIV-1 particle production and the enhancement of Gag association with microtubules [11]. The mechanism by which SOCS1 inhibits cytokine signaling is mediated by the inhibition of kinase activity through its N-terminal kinase inhibitory region (KIR) [18]. We next examined whether SOCS1 mutants lacking the function of either KIR (SOCS1-F59D) or SOCS-box (ΔSOCS) affected virus particle production. Our ELISA results indicate that the SOCS-box deletion mutant (ΔSOCS) of SOCS1 fails to promote virus production, whereas the KIR mutant, F59D, of SOCS1 partially enhances HIV-1 particle production when co-transfected with pNL4-3 in 293T cells (Fig. 5A and B). These data again suggest that the function of SOCS1 in HIV-1 particle production is not principally due to the suppression of interferon/cytokine signaling, but is mediated by its direct interaction with the HIV-1 Gag via the function of the SOCS-box.

The SOCS-box-mediated function of SOCS1 is chiefly exerted via its ubiquitin ligase activity [19]. Indeed, several reports have demonstrated that Gag ubiquitination is related to its membrane association and particle release, although the function of HIV-1 Gag ubiquitination remains unclear [20,21]. We thus explored the possibility that SOCS1 modulates the ubiquitination of HIV-1 Gag, leading to enhanced virus particle formation. We initially examined the specific interaction of HIV-1 Gag with the SOCS1-E3 ligase complex. Purified SOCS1 and its E3 component proteins (biotinylated-Cullin 2, elongin B/C and Rbx1) in addition to HIV-1 Gag were synthesized in a wheat germ cell-free system and then subjected to pull-down assays using streptavidin coated magnetic beads. We found that Gag was co-purified with a SOCS1-E3 complex comprising SOCS1-elongin B/C-Rbx1-Cullin2 in a similar manner to RelA, a previously reported SOCS1 binding protein (Fig. 5C, left). Significantly, in the absence of SOCS1, both elongin B and C were not co-purified with Cullin 2 probably due to the unsteady condition of the E3 complex without SOCS1, and the amount of bound Gag was also reduced (Fig. 5C, right).These result indicate that the SOCS1-E3 complex associates with HIV-1 Gag and may promote its ubiquitination.

We next addressed whether SOCS1 affects the ubiquitination of HIV-1 Gag. Immunoprecipitation analysis with cells co-transfected with Gag-FLAG and myc-tagged ubiquitin, with or without SOCS1 co-transfection, revealed that SOCS1 overexpression significantly enhances the ubiquitination of the Gag protein (Fig. 5D). In contrast, the targeted depletion of SOCS1 by siRNA significantly reduced the amount of ubiquitinated Gag (Fig. 5E). These results indicate that SOCS1 could indeed be a potent ubiquitin ligase for HIV-1 Gag.

To clarify the biological significance of Gag ubiquitination via SOCS1, we performed an experiment using a dominant-negative ubiquitin construct lacking two C-terminal glycines (residues 75–76). This mutant ubiquitin (UbΔGG) cannot become conjugated to target substrates, but can bind noncovalently to ubiquitin interacting domains [14]. By immunoprecipitation analysis we revealed that the levels of HIV-1 Gag associated with microtubules were significantly reduced in cells expressing UbΔGG, as compared with those expressing wild-type ubiquitin (Ub-WT) (Fig. 5F). This trend was further revealed by a microtubule sedimentation experiment showing that the expression of UbΔGG reduced the amount of Gag associated with microtubules when compared with the expression of Ub-WT (Fig. 5G). These results together indicate a link between ubiquitin signaling and the microtubule-mediated Gag dynamics involved with HIV-1 particle formation.

4. Discussion

In our current study, we report that microtubule integrity is required for SOCS1 to facilitate Gag trafficking and virus particle production. We demonstrate from our experiments that (1) SOCS1 colocalizes with HIV-1 Gag along microtubules; (2) both SOCS1 and HIV-1 Gag are co-purified with microtubules and SOCS1 can augment the association of Gag with microtubules; (3) an intact microtubule network is required for the function of SOCS1 during Gag trafficking; (4) SOCS1 facilitates Gag ubiquitination; and (5) Gag association with the microtubules is significantly reduced when a dominant-negative Ub mutant is overexpressed. These results together indicate that SOCS1 can regulate the trafficking and stability of HIV-1 Gag via the microtubule-related cellular machinery, which may be in turn enhanced by Gag ubiquitination.

SOCS1 was identified initially as a negative regulator of signaling downstream of cytokines [22–24] and has been shown to localize at both the perinuclear region and the microtubule organizing center (MTOC) in cells [16]. We show from our current data that SOCS1 also forms dotted filamentous structures in the cytoplasm emanating from the perinuclear region, including the MTOC, to the cell periphery. A recent report has also indicated that Gag colocalizes at the MTOC with HIV-1 RNA and is subsequently transported to the cell periphery [25]. These observations together indicate that SOCS1 might facilitate the trafficking of HIV-1 Gag from the MTOC toward the plasma membrane by utilizing the intrinsic transport machinery of infected host cells.

The plus-end directed transport system along the microtubules could provide a means for the targeting of virus capsid proteins to the site of virus assembly and budding in the vicinity of the plasma membrane [26]. This ante-grade transport system is utilized by several viruses, such as herpes simplex virus type 1 (HSV-1), vaccinia virus and African swine fever virus (ASFV) [26–29]. Significantly, we have demonstrated in our present study that HIV-1 can utilize the microtubule-dependent transport mechanism, which may in turn be enhanced by SOCS1. Consistent with this notion, Leblanc et al. have demonstrated previously using a monoclonal antibody raised against unprocessed Gag that intracellular Gag puncta can travel along microtubules [30]. Our current microtubule pull-down analyses also clearly indicate that SOCS1 associates with Gag on microtubules and can enhance this interaction. This in turn might accelerate the intracellular trafficking of Gag to the plasma membrane along these structures, although the topological details are still unknown. Consistent with this observation, a plus-end microtubule motor KIF4 has been shown previously to associate with HIV-1 Gag and to enhance Gag trafficking [31,32]. These results further demonstrate the relevance of microtubule network in the trafficking of the HIV-1 Gag.

The involvement of the microtubule cytoskeleton in Gag assembly and HIV-1 particle egress is somewhat controversial [3,26,33,34]. However, several reports have presented convincing data to indicate the importance of this network in HIV-1 assembly